Effects of Backbone Rigidification on Intramolecular Hydrogen Bonding in a Family of Diamides†

Gui-Bai Liang, John M. Desper, and Samuel H. Gellman*

Contribution from the S. M. McElvain Laboratory of Organic Chemistry, Department of Chemistry, University of Wisconsin, 1101 University Avenue, Madison, Wisconsin 53706.
Received August 7, 1992

Abstract: In an effort to gain insight on the balance of noncovalent forces that controls the adoption of folded conformations in small molecules, we have examined intramolecular hydrogen bond formation in a series of diamides containing a variety of conformational constraints. The intramolecularly hydrogen-bonded state of flexible diamide **2** was previously shown to be enthalpically favored by about 1.5 kcal/mol relative to the non-hydrogen-bonded state in methylene chloride. For flexible diamide **1**, however, the enthalpic preference for the intramolecularly hydrogen-bonded state is only about 0.4 kcal/mol in this solvent. We describe here the synthesis and behavior of diamides **3–9**, in which eight- or nine-membered-ring N—H···O=C hydrogen bonds occur in rigidified frameworks. Thermodynamic parameters were determined spectroscopically for the two-state equilibrium, non-hydrogen-bonded vs intramolecularly hydrogen-bonded, for diamides **3** and **4** in methylene chloride. The intramolecularly hydrogen-bonded state of **3** is enthalpically favored by ca. 1.6 kcal/mol. The enhanced enthalpic favorability of the internally hydrogen-bonded state of **3**, relative to **1**, is consistent with the MM2/MacroModel prediction that formation of an optimal hydrogen bond by **1** requires an eclipsed torsion angle in the linking segment. The intramolecularly hydrogen-bonded state of **4** is enthalpically favored by about 1.1 kcal/mol. The diminished enthalpic favorability relative to **3** may result from the poorer hydrogen-bond-accepting ability of the lactam carbonyl, relative to the acyclic tertiary carbonyl of **3**. The extent of intramolecular hydrogen bonding in **5** is less than or equal to the extent in **2** at all temperatures in methylene chloride. Among the olefinic series **6–8**, the addition of methyl substituents to the alkene carbons is found to promote hydrogen bond formation so effectively that **8** is predominantly hydrogen bonded in acetonitrile at room temperature, conditions under which little or no intramolecular hydrogen bonding can be detected for **1** or **6**. X-ray diffraction data show that the intramolecular hydrogen bond is maintained by **8** in the solid state.

Introduction

The tendencies of diamides **1** and **2** to adopt intramolecularly hydrogen-bonded conformations in methylene chloride are quite different from one another.[1] Variable-temperature ^{1}H NMR and IR data indicate that the nine-membered-ring hydrogen-bonded state of **2** is approximately 1.5 kcal/mol more favorable enthalpically than the non-hydrogen-bonded state.[1] For **1**, however, variable-temperature IR data imply that the eight-membered-ring hydrogen-bonded state is only ca. 0.4 kcal/mol enthalpically favored over the non-hydrogen-bonded state.[2] Molecular mechanics calculations suggest that both ring sizes can accommodate an N—H···O=C interaction of optimal geometry; therefore, the more enthalpically favorable hydrogen bonding in the larger ring probably reflects differences in torsional strain and other nonbonded interactions that develop as the amide groups approach one another.

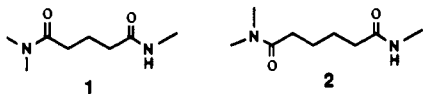

1 **2**

The two spectroscopically defined conformational states for **1** and **2** in dilute solution, non-hydrogen-bonded[3] and intramolecularly hydrogen-bonded, may each comprise a number of discrete conformations. We would like to identify those conformations most conducive to hydrogen bond formation in order to gain insight on the balance of noncovalent forces that controls the adoption of compact forms in these small molecules, and to provide a basis for the design of new polymeric systems that will fold in defined ways.[4] Described here is the behavior of diamides **3–9**, in which eight- and nine-membered hydrogen-bonded rings occur in conformationally restricted frameworks.[5] Differences in the extent of formation of a single N—H···O=C hydrogen bond among these diamides reveal the relative tendencies of the hydrocarbon linking segments to adopt folded conformations.

As in our previous study of **1** and **2**, we have employed both IR and NMR methods to analyze the solution behavior of the new diamides. IR spectroscopy is particularly useful for examining intramolecular hydrogen bonding in these diamides because equilibration between intramolecularly hydrogen-bonded and non-hydrogen-bonded[3] states is slow on the IR time scale; thus, for each diamide, these two states give rise to distinct NH stretch bands in a nonpolar solvent. On the ^{1}H NMR time scale, in contrast, hydrogen-bond equilibration is rapid, and the observed resonances are weighted averages of the contributing hydrogen-bonded and non-hydrogen-bonded states. Nevertheless, it is

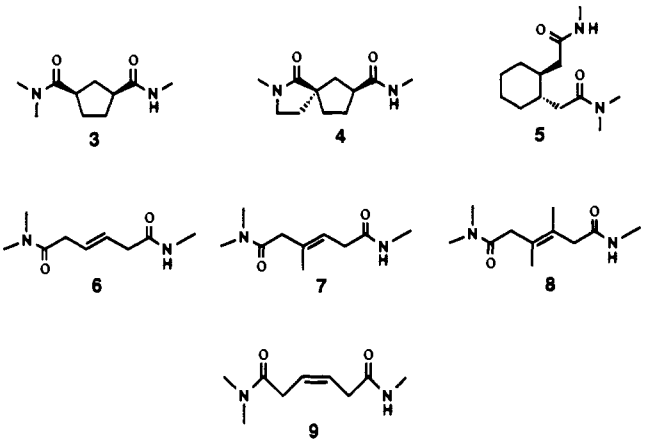

3 **4** **5** **6** **7** **8** **9**

† Dedicated to Professor Ralph Hirschmann on the occasion of this 70th birthday.

(1) Gellman, S. H.; Dado, G. P.; Liang, G.-B.; Adams, B. R. *J. Am. Chem. Soc.* **1991**, *113*, 1164.

(2) The thermodynamic parameters for **1** were derived from data described in ref 1.

(3) We use the term "non-hydrogen-bonded" to signify the absence of a strong N—H···O=C interaction in methylene chloride solution. Such amide protons are presumably involved in weakly attractive dipole–dipole interactions with the solvent.

(4) For related efforts on unnatural oligoamide backbones, see: (a) Nowick, J. S.; Powell, N. A.; Martinez, E. J.; Smith, E. M.; Noronha, G. *J. Org. Chem.* **1992**, *57*, 3763. (b) Hagihara, M.; Anthony, N. J.; Stout, T. J.; Clardy, J.; Schreiber, S. L. *J. Am. Chem. Soc.* **1992**, *114*, 6568.

(5) Some properties of **6** and **8** have been described in a preliminary communication: Liang, G.-B.; Dado, G. P.; Gellman, S. H. *J. Am. Chem. Soc.* **1991**, *113*, 3994.

0002-7863/93/1515-925$04.00/0

common to try to elucidate hydrogen-bonding behavior in peptides on the basis of amide proton NMR data,[6] because the presence of multiple NH groups (specifically, the resulting band overlap) often renders IR data inconclusive in such cases. Spectroscopic correlations for relatively simple diamides establish guidelines for the interpretation of NMR data obtained for more complex molecules. Indeed, our recent correlations between NMR and IR data[1] have shown that previous attempts to analyze intramolecular hydrogen-bonding behavior in flexible peptides on the basis of variable-temperature NMR data have involved overly simplistic assumptions.

Results

Computational Attempts To Identify the Minimum Energy Conformations of Diamides 1 and 2. We used molecular mechanics methods to try to identify the most favorable intramolecularly hydrogen-bonded conformations of **1** and **2**, employing the "multiconformer" mode of MacroModel v3.0.[7] Starting geometries for each diamide were generated by varying all single bonds between the two amide groups of each molecule (four C–C bonds for **1**, five for **2**), with the distance from the amide proton to the tertiary amide oxygen constrained to be between 1 and 3 Å. Separate multiconformer searches were carried out for **1** and **2** with the MM2,[8] AMBER,[9] and OPLSA[10] force fields, as implemented by MacroModel v3.0.[7]

For **1**, the lowest energy conformation found by AMBER was similar to that found by OPLSA; each had both of the CH_2—CH_2 bonds gauche (g^+g^+) and an N—H···O=C interaction of good geometry. (Criteria for good N—H···O=C hydrogen-bonded geometry were as follows: distance ≤ 2.0 Å; N—H···O angle ≥ 150°; C=O···H angle ≥ 100°; and secondary amide proton in or near the plane defined by the tertiary amide N—C=O unit.[11]) The lowest energy conformation found by MM2 had one backbone CH_2—CH_2 nearly eclipsed and a hydrogen bond of good geometry. For **2**, the AMBER and OPLSA minimum energy structures were again similar to one another, with all three CH_2—CH_2 bonds gauche (torsion angle sequence: $g^+g^-g^-$). The N—H···O=C geometry in these two minimum energy conformations was poor because the proton approached the tertiary amide oxygen from well outside the N—C=O plane. The lowest energy MM2 conformation was quite different, with the central CH_2—CH_2 anti, the other two CH_2—CH_2 bonds gauche (torsion angle sequence: g^+ag^-), and a good hydrogen bond geometry.

Rigidification Targets. Using the computational results above for qualitative guidance, we identified diamides **3–9** as molecules likely to experience increased hydrogen bonding, relative to **1** and **2**, in eight- and/or nine-membered rings. The 1,3-cyclopentyl linking segment of **3** was chosen on the basis of the MM2 results indicating that eclipsing interactions might be required for an optimal intramolecular hydrogen-bonding interaction in **1**. Low energy conformations of cyclopentane itself contain unavoidable eclipsing interactions,[12] so it seemed likely that the occurrence of eclipsed torsion angles would not disfavor internally hydrogen-bonded states of **3** relative to non-hydrogen-bonded states. The rigidified backbone of diamide **3** also seemed likely to reduce the conformational entropy cost of hydrogen-bond formation; spiro lactam **4** was targeted in an attempt to reduce this conformational entropy cost even further.

Diamide **5** was selected as a rigidified analogue of **2** in which the *trans*-1,2-disubstituted cyclohexyl linker would constrain the central CH_2—CH_2 bond to a gauche torsion angle, as predicted to be optimal by AMBER and OPLSA. Olefinic diamides **6–8** were chosen on the basis of the MM2 suggestion that the central CH_2—CH_2 bond is anti in the most stable intramolecularly hydrogen-bonded conformation of **2**. Conformational analysis of 1-butene indicates that the conformer in which the CH_2—CH_3 bond eclipses the CH=CH_2 bond is at or near the global energy minimum.[13] Therefore, even though the central C=C bond of **6** is constrained to be anti, the presence of the double bond may

Scheme I[a]

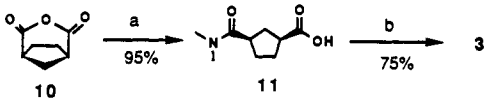

[a] Reagents: (a) aqueous Me_2NH; (b) DCC, HOSu; $MeNH_2$.

Scheme II[a]

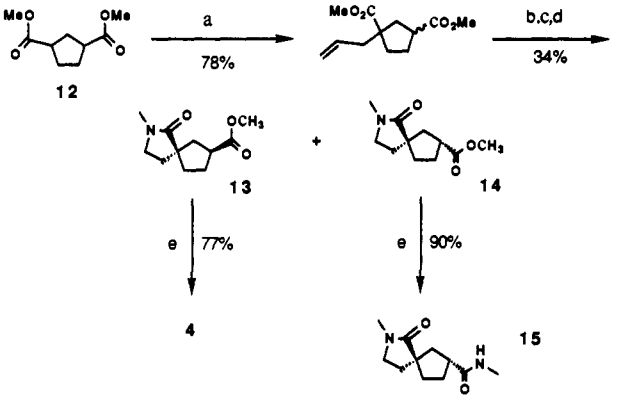

[a] Reagents: (a) LDA, THF; H_2C=$CHCH_2Br$; (b) O_3; (c) $MeNH_2$, $NaBH_3CN$; (d) $iPrNH_2$, MeOH; (e) $MeNH_2$, NaCN, MeOH.

Scheme III[a]

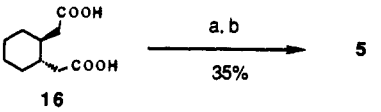

[a] Reagents: (a) CH_3COCl; aqueous Me_2NH; (b) DCC, HOSu; $MeNH_2$.

Scheme IV[a]

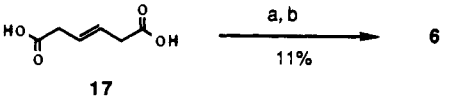

[a] Reagents: (a) CH_3COCl; aqueous Me_2NH; (b) DCC, HOSu; $MeNH_2$.

Scheme V[a]

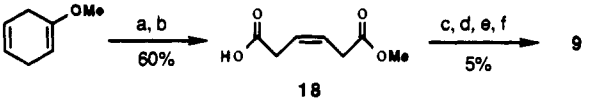

[a] Reagents: (a) O_3; (b) Jones oxidation; (c) oxalyl chloride; (d) Me_2NH; (e) KOH; (f) DCC, HOSu; $MeNH_2$.

(6) For leading references, see: (a) Rose, G. D.; Gierasch, L. M.; Smith, J. A. *Adv. Protein Chem.* **1985**, *37*, 1. (b) Kessler, H. *Angew. Chem., Int. Ed. Engl.* **1982**, *21*, 512. (c) Stevens, E. S.; Sugawara, N.; Bonora, G. M.; Toniolo, C. *J. Am. Chem. Soc.* **1980**, *102*, 7048.

(7) (a) Mohamdi, F.; Richards, N. G. J.; Guida, W. C.; Liskamp, R.; Lipton, M.; Caufield, C.; Chang, C.; Chang, G.; Hendrickson, T.; Still, W. C. *J. Comput. Chem.* **1990**, *11*, 440. (b) Lipton, M.; Still, W. C. *J. Comput. Chem.* **1988**, *9*, 343.

(8) Burkert, U.; Allinger, N. L. *Molecular Mechanics*; ACS Monograph Series 177; American Chemical Society: Washington, DC, 1982.

(9) Weiner, S.; Kollman, P. A.; Nguyen, D. T.; Case, D. A. *J. Comput. Chem.* **1986**, *7*, 230.

(10) Jorgensen, W. L.; Tirado-Rives, J. *J. Am. Chem. Soc.* **1988**, *110*, 1657.

(11) Baker, E. R.; Hubbard, R. E. *Prog. Biophys. Mol. Biol.* **1984**, *44*, 97 and references therein. See especially p 144.

(12) Eliel, E. L.; Allinger, N. L.; Angyal, S. J.; Morrison, G. A. *Conformational Analysis*; Wiley-Interscience: New York, 1965; and references therein.

(13) (a) Kondo, S.; Hirota, E.; Morino, Y. *J. Mol. Spectrosc.* **1968**, *28*, 471. (b) Harmony, M. D.; Laurie, V. W.; Kuckowski, R. L.; Schwendeman, R. H.; Ramsey, D. A.; Lovas, F. J.; Lafferty, W. J.; Maki, A. G. *J. Phys. Chem. Ref. Data* **1979**, *8*, 619. (c) Durig, J. R.; Compton, D. A. *J. Phys. Chem.* **1980**, *84*, 773.

Scheme VI[a]

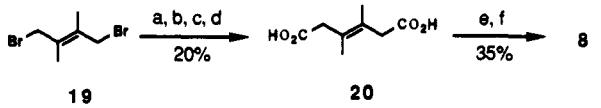

[a] Reagents: (a) 2-Lithio-1,3-dithiane; (b) $PhI(O_2CCF_3)_2$, MeOH; (c) pTsOH, aqueous THF; (d) Jones oxidation; (e) DCC; aqueous Me_2NH; (f) DCC, HOSu; $MeNH_2$.

Scheme VII[a]

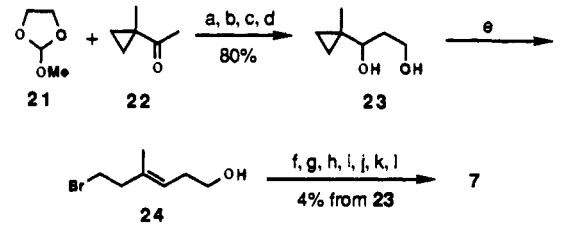

[a] Reagents: (a) BF_3·OEt_2; iPr_2NEt; (b) $LiAlH_4$; (c) aqueous HCl, THF; (d) $NaBH_4$; (e) $MgBr_2$, Et_2O; aqueous HBr; (f) AcOCs, DMF; (g) Jones oxidation; (h) H_2SO_4, MeOH; (i) Jones oxidation; (j) DCC, HOSu; Me_2NH; (k) aqueous KOH; (l) DCC, HOSu; $MeNH_2$.

predispose the carbonyl carbons to lie in the plane defined by the C—C=C—C unit, which is antithetical to intramolecular hydrogen-bond formation. The additional methyl groups of **7** and **8** were intended to force one or both of the carbonyl carbons to reside above or below the C—C=C—C plane[14] (avoidance of $A^{(1,2)}$ and $A^{(1,3)}$ strain[15]), thereby promoting internal N—H···O=C interaction. Diamide **9** was examined in order to compare the effects of cis and trans conformations about the central C=C bond on hydrogen bond formation in the nine-membered ring.

Synthesis of Rigidified Diamides. Diamide **3** was prepared from anhydride **10**[16] via amide acid **11** (Scheme I). Scheme II shows the preparation of spiro lactam **4**. Monoalkylation of dimethyl *cis*-cyclopentane-1,3-dicarboxylate[17] (**12**) proceeded smoothly under controlled conditions, and the product, as a mixture of epimers, was carried on through a three-step sequence to provide the chromatographically separable isomeric spiro lactam esters **13** and **14**. These isomers were converted individually to **4** and its epimer **15**; the latter proved to be useful as a spectroscopic reference. Diamide **5** was prepared from diacid **16**[18] in a route that involved polymeric anhydride formation, as shown in Scheme III.

The synthesis of olefinic diamide **6** from commercially available diacid **17** also involved the intermediacy of a polymeric anhydride (Scheme IV). Scheme V shows the preparation of the cis isomer, **9**. Alkene stereochemistry was established via selective ozonolytic ring opening of 2,5-dihydroanisole[19] which, after Jones oxidation in situ, provided acid ester **18**. As indicated in Scheme VI, the trans stereochemistry of tetrasubstituted olefinic diamide **8** was derived from that of the known dibromide **19**.[20] The requisite carboxyl groups were added via displacement with 2-lithio-1,3-dithiane, followed by deprotection and oxidation. Diacid **20** was converted to diamide **8** by way of a polymeric anhydride.

Diamide **7** presented a particular challenge, because the lack of symmetry in the parent diacid precluded the intermediacy of a polymeric anhydride (we assumed that it would be difficult or impossible to separate **7** from the isomer that would necessarily result from such an approach). Scheme VII shows a route that incorporates the highly trans-selective Julia–Johnson olefination[21] as a key step. Lewis acid-catalyzed aldol-like condensation of commercially available **21** and **22** was followed by ketone reduction, acetal hydrolysis, and aldehyde reduction, providing diol **23** in 80% overall yield. The bromide resulting from the olefination procedure, **24**, was immediately converted to the corresponding acetate. This acetate was converted to **7** in 12% overall yield via a sequence of standard functional group manipulations. As indicated in the Experimental Section, product stereochemistry was established by a series of NOE measurements on a derivative of an advanced intermediate.

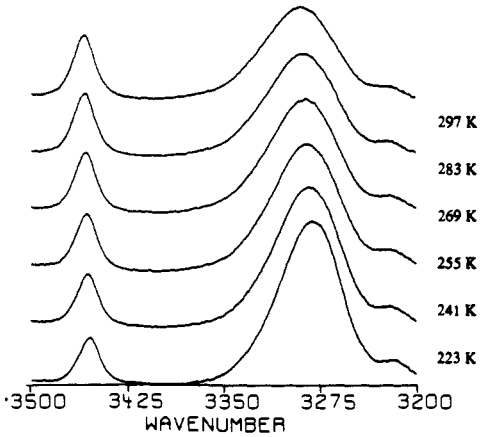

Figure 1. NH stretch region of FT-IR spectral data for 1 mM diamide **3** in CH_2Cl_2, as a function of temperature, after subtraction of the spectrum of pure CH_2Cl_2 at the same temperature. Absorption maxima at 297 K: 3459 (non-hydrogen-bonded) and 3292 cm^{-1} (intramolecularly hydrogen-bonded).

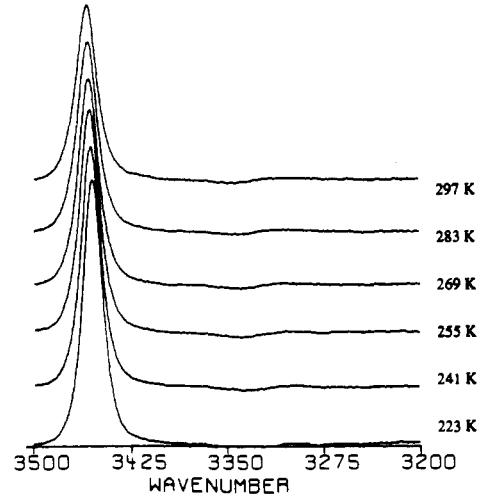

Figure 2. NH stretch region the FT-IR spectral data for 1 mM amide **25** in CH_2Cl_2, after subtraction of the spectrum of pure CH_2Cl_2 at the same temperature. Absorption maximum at 297 K: 3459 cm^{-1} (non-hydrogen-bonded).

Variable-Temperature Spectroscopic Data for 3–5. Figure 1 shows variable-temperature FT-IR data from the NH stretch region for a 1 mM solution of **3** in CH_2Cl_2, 223–297 K, after subtraction of pure solvent at the appropriate temperature (little or no aggregation occurs under these conditions, as indicated by experiments described below). The room-temperature spectrum shows a large absorption at 3292 cm^{-1}, which may be attributed to an intramolecularly hydrogen-bonded NH moiety, and a smaller band at 3459 cm^{-1}, which may be attributed to an NH moiety interacting with the solvent. In contrast, diamide **1** shows only

(14) For a recent review on torsional barriers associated with variously substituted sp^3–sp^2 bonds, see: Berg, U.; Sandström, J. *Adv. Phys. Org. Chem.* **1989**, *25*, 1. For discussions of the effects of these conformational preferences on reactivity, see: (a) Broeker, J. L.; Hoffmann, R. W.; Houk, K. N. *J. Am. Chem. Soc.* **1991**, *113*, 5006. (b) Clennan, E. L.; Chen, X.; Koola, J. J. *J. Am. Chem. Soc.* **1990**, *112*, 5193.

(15) (a) Johnson, F. *Chem. Rev.* **1968**, *68*, 375. (b) Hoffmann, R. W. *Angew. Chem., Int. Ed. Engl.* **1992**, *31*, 1124.

(16) Playtis, A. J.; Fessekis, J. D. *J. Org. Chem.* **1975**, *40*, 2488.

(17) Weagley, R. J.; Gibson, H. W. *Synthesis* **1986**, 552.

(18) Stork, G.; Darling, S. D. *J. Am. Chem. Soc.* **1964**, *86*, 1761.

(19) Corey, E. J.; Katzenellenbogen, J. A.; Gilman, N. M.; Roman, S. A.; Erickson, B. W. *J. Am. Chem. Soc.* **1968**, *90*, 5618.

(20) Murray, R. W.; Agarwal, S. K. *J. Org. Chem.* **1985**, *50*, 4698.

(21) Brady, S. F.; Ilton, M. A.; Johnson, W. S. *J. Am. Chem. Soc.* **1968**, *90*, 2882.

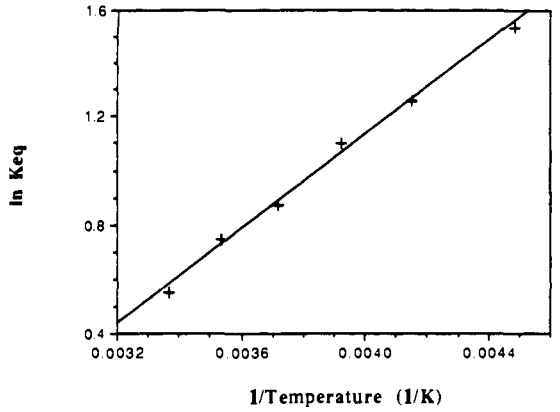

Figure 3. Representative van't Hoff plot constructed from NH stretch region FT-IR data for 1 mM diamide **3** in CH_2Cl_2, 223–297 K, using data from amide **25** to provide the integrated extinction coefficient for the non-hydrogen-bonded NH stretch, as described in the text. The line represents the best fit to the equation $\ln K_{eq} = -\Delta H°/RT + \Delta S°/R$, with $\Delta H°$ = −1.7 kcal/mol and $\Delta S°$ = −4.7 eu (correlation coefficient = 0.995).

Table I. IR-Based Thermodynamic Parameters for Non-Hydrogen-Bonded vs Intramolecularly Hydrogen-Bonded States of Diamides **1**–**4** in CH_2Cl_2

diamide	$\Delta H°$ (kcal/mol)[a]	$\Delta S°$ (eu)[b]
1[c]	−0.4	−3.3
2[d]	−1.5	−7.5
3	−1.6	−4.4
4	−1.1	−2.8

[a] The $\Delta H°$ values are estimated to be accurate to ±0.2 kcal/mol. [b] The $\Delta S°$ values are estimated to be accurate to ±1 eu. [c] The values for **1** were obtained from analysis of data described in ref 1. [d] Values for **2** were taken from ref 1.

a very small hydrogen-bonded NH band, at 3320 cm^{-1}, under these conditions.[1] Despite the increased hydrogen bonding in **3** relative to **1**, however, the CH_2Cl_2 solution of **3** contains significant populations of the non-hydrogen-bonded state at all temperatures (ca. 36% at 297 K and ca. 18% at 223 K).

The variable-temperature IR data in Figure 1 were used to determine the thermodynamic relationship between non-hydrogen-bonded and intramolecularly hydrogen-bonded states of **3** in CH_2Cl_2. The methyl amide of cyclopentanecarboxylic acid, **25**, shows only a single, non-hydrogen-bonded, NH stretch signal throughout the temperature range (Figure 2), suggesting that aggregation does not occur under these conditions. The data for

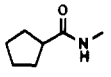

25

this monoamide were used to define the integrated extinction coefficient (3400–3500 cm^{-1}) for diamide **3** as a function of temperature. This integrated extinction coefficient allowed us to calculate the concentration of non-hydrogen-bonded NH moieties in the 1 mM solution of **3** at various temperatures from the data shown in Figure 1. Since we also knew the total concentration of **3**, we could deduce the concentration of intramolecularly hydrogen-bonded NH groups as that portion of the total amide concentration not accounted for by the non-hydrogen-bonded portion. (It was not possible to determine the concentration of intramolecularly hydrogen-bonded NH moieties directly from the low energy band in the spectra shown in Figure 1, because we lacked a fully hydrogen-bonded model compound that would have allowed us to estimate the temperature-dependent integrated extinction coefficient of this band.)

Assuming that the behavior of **3** could be treated according to a two-state model, non-hydrogen-bonded vs intramolecularly hydrogen-bonded (eq 1), we used eq 2 and the IR-derived equilibrium constants to determine the enthalpic and entropic relationship between these two states. A typical van't Hoff plot is shown in Figure 3. On the basis of duplicate data sets for both

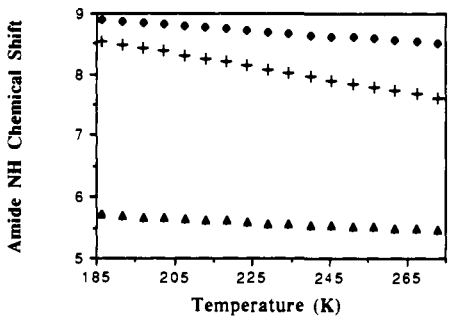

Figure 4. Amide proton NMR chemical shifts as a function of temperature (data sets used to determine van't Hoff $\Delta H°$ and $\Delta S°$, as described in the text): 1 mM diamide **3** in CD_2Cl_2 (+); 1 mM each *N*-methylacetamide and *N*,*N*-dimethylacetamide in CD_2Cl_2, used as reference for the non-hydrogen-bonded state (▲); $\Delta\delta NH/\Delta T$ signature passing through 8.40 ppm at 295 K with a slope of 5.0×10^{-3} ppm/K, used as reference for the fully intramolecularly hydrogen-bonded state (see ref 1) (◆).

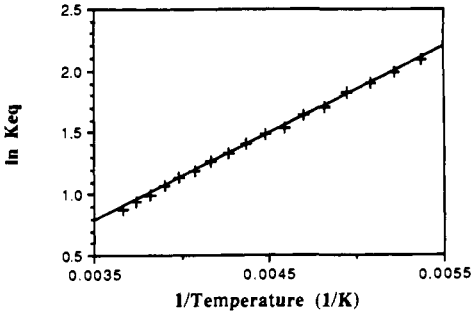

Figure 5. van't Hoff plot for non-hydrogen-bonded vs intramolecularly hydrogen-bonded **3**, from amide proton NMR data obtained with 1 mM samples in CD_2Cl_2, 185–275 K (Figure 4). $K_{eq} = (\delta_{obsd} - \delta_n)/(\delta_b - \delta_{obsd})$, where δ_{obsd} is the chemical shift of the amide proton of **3** at that temperature, δ_n is the chemical shift of the amide proton in a solution containing 1 mM each of *N*-methylacetamide and *N*,*N*-dimethylacetamide at that temperature, and δ_b is given by the $\Delta\delta/\Delta T$ function passing through 8.40 ppm at 295 K with a slope of -5.0×10^{-3} ppm/K (ref 1). The line represents the best fit to the equation $\ln K_{eq} = -\Delta H°/RT + \Delta S°/R$, with $\Delta H°$ = −1.4 kcal/mol and $\Delta S°$ = −3.4 eu (correlation coefficient = 0.999).

3 and **25**, we conclude that the internally hydrogen-bonded state of **3** in CH_2Cl_2 is enthalpically favored over the non-hydrogen-bonded state by 1.6 kcal/mol, but entropically disfavored by 4.4 eu. (IR-derived thermodynamic parameters are summarized in Table I.)

$$3(\text{non-HB}) \overset{K_{eq}}{\rightleftharpoons} 3(\text{intramolecularly HB}) \quad (1)$$

$$\ln K_{eq} = -(\Delta H°/RT) + \Delta S°/R \quad (2)$$

In our original study, we were able to use variable-temperature ^1H NMR measurements ($\Delta\delta NH/\Delta T$) to obtain $\Delta H°$ and $\Delta S°$ for the equilibrium between non-hydrogen-bonded and hydrogen-bonded states of **2** in methylene chloride.[1] Good correlation between these NMR-derived thermodynamic values and IR-derived values was observed when $\Delta\delta NH/\Delta T$ data from a solution containing 1 mM *N*-methylacetamide and 1 mM *N*,*N*-dimethylacetamide were used to represent the limiting non-hydrogen-bonded state (δ_n) and a $\Delta\delta NH/\Delta T$ signature passing through 8.4 ppm at 295 K with a slope of -5.0×10^{-3} ppm/K was used to represent the limiting intramolecularly hydrogen-bonded state (δ_b).[1,22] We carried out a similar analysis for diamide

(22) The use of a relatively large negative temperature dependence for the fully intramolecularly hydrogen-bonded state (−5.0 ppm/K) contrasts with the common assumption that in nonpolar solvents fully hydrogen-bonded states are characterized by smaller $\Delta\delta NH/\Delta T$ values (see ref 6). Adrian and Wilcox have recently reported an intermolecularly hydrogen-bonded limiting state that shows a $\Delta\delta NH/\Delta T$ of −6.6 ppm/K: Adrian, J. C.; Wilcox, C. S. *J. Am. Chem. Soc.* **1991**, *113*, 678.

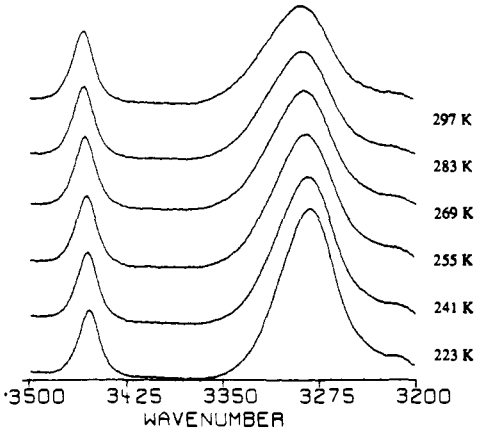

Figure 6. NH stretch region of FT-IR spectral data for 1 mM spiro lactam **4** in CH_2Cl_2, as a function of temperature, after subtraction of the spectrum of pure CH_2Cl_2 at the same temperature. Absorption maxima at 297 K: 3459 (non-hydrogen-bonded) and 3290 cm^{-1} (intramolecularly hydrogen-bonded).

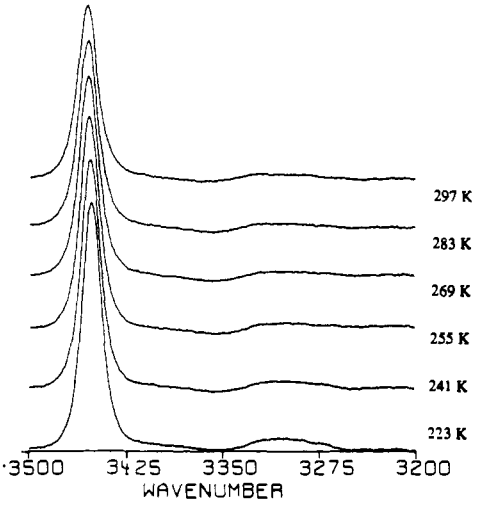

Figure 7. NH stretch region of FT-IR spectral data for 1 mM amide **15** in CH_2Cl_2, after subtraction of the spectrum of pure CH_2Cl_2 at the same temperature. Absorption maximum at 297 K: 3456 cm^{-1} (non-hydrogen-bonded).

3, using $\Delta\delta NH/\Delta T$ data obtained with a 1 mM sample of **3** in CD_2Cl_2. Figure 4 shows the $\Delta\delta NH/\Delta T$ signatures used for this analysis. At each temperature, the equilibrium constant (defined in eq 1) is obtained from the NMR data by eq 3, where δ_{obsd} is

$$K_{eq} = (\delta_{obsd} - \delta_n)/(\delta_b - \delta_{obsd}) \quad (3)$$

the chemical shift measured for **3** at a given temperature, δ_n is the chemical shift of the monoamide mixture at that temperature, representing the limiting non-hydrogen-bonded state, and δ_b is the chemical shift given by the $\Delta\delta NH/\Delta T$ function used to represent the limiting hydrogen-bonded state, at that temperature. The resulting K_{eq} values were used to construct a van't Hoff plot (Figure 5). This analysis implies that the intramolecularly hydrogen-bonded state of **3** is enthalpically favored by 1.4 kcal/mol, but entropically disfavored by 3.4 eu in CD_2Cl_2. The relatively small differences between the independent NMR-derived and IR-derived $\Delta H°$ and $\Delta S°$ values provide an estimate of the accuracy of the thermodynamic parameters.

A $\Delta\delta NH/\Delta T$ data set obtained with a 10 mM solution of **3** in CD_2Cl_2 was used to carry out a parallel thermodynamic analysis with the δ_n and δ_b functions described above. The resulting van't Hoff plot (not shown) indicated that the intramolecularly hydrogen-bonded state was enthalpically favored by 1.5 kcal/mol, but entropically disfavored by 3.7 eu. The agreement between these values and the values derived using data obtained with 1 mM **3** indicates that aggregation is not significant in the 1 mM solution.

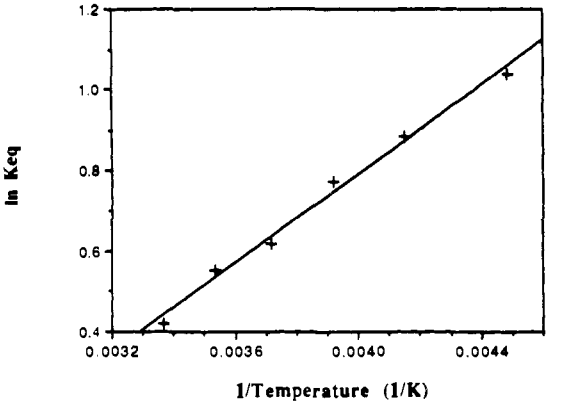

Figure 8. Representative van't Hoff plot constructed from NH stretch region of FT-IR data for 1 mM spiro lactam **4** in CH_2Cl_2, 223–297 K, using data from amide **15** to provide the integrated extinction coefficient for the non-hydrogen-bonded NH stretch, as described in the text. The line represents the best fit to the equation $\ln K_{eq} = -\Delta H°/RT + \Delta S°/R$, with $\Delta H° = -1.1$ kcal/mol and $\Delta S° = -2.2$ eu (correlation coefficient = 0.990).

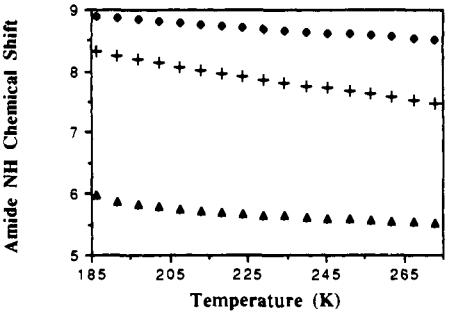

Figure 9. Amide proton NMR chemical shifts as a function of temperature (data sets used to determine van't Hoff $\Delta H°$ and $\Delta S°$, as described in the text): 1 mM diamide **4** in CD_2Cl_2 (+); 1 mM lactam **15** in CD_2Cl_2, used as reference for the non-hydrogen-bonded state (▲); $\Delta\delta NH/\Delta T$ signature used as reference for the fully intramolecularly hydrogen-bonded state (see ref 1) (◆).

Figure 6 shows variable-temperature IR data from the NH stretch region for a 1 mM solution of **4** in CH_2Cl_2. These spectra are qualitatively similar to those obtained for **3** (Figure 1), showing a major band for an internally hydrogen-bonded NH moiety and a minor but significant band for a non-hydrogen-bonded NH moiety (3459 and 3290 cm^{-1}, respectively, at room temperature). Figure 7 shows analogous data for epimer **15**, which indicate that little or no aggregation occurs under these conditions. The data in Figure 7 were used to determine the temperature-dependent integrated extinction coefficient for the non-hydrogen-bonded NH stretch band. On the basis of duplicate data sets for both **4** and **15**, we conclude that the internally hydrogen-bonded state is enthalpically favored by 1.1 kcal/mol but entropically disfavored by 2.8 eu, relative to the non-hydrogen-bonded state (Figure 8 shows a representative van't Hoff plot).

An NMR-based thermodynamic analysis of the two-state behavior of **4** was carried out in a manner similar to the NMR-based analysis of **3**, except that $\Delta\delta NH/\Delta T$ data for epimeric spiro lactam **15** were used to model the non-hydrogen-bonded limiting state. Figure 9 shows the $\Delta\delta NH/\Delta T$ data for **4** and **15** and the $\Delta\delta NH/\Delta T$ signature used to represent the fully hydrogen-bonded limiting state. The van't Hoff analysis (Figure 10) implies that the intramolecularly hydrogen-bonded state of **4** is 0.9 kcal/mol more favorable enthalpically but 1.8 eu less favorable entropically than the non-hydrogen-bonded state, in methylene chloride. As was the case for **3**, the NMR-based and IR-based thermodynamic analyses agree reasonably well with one another, particularly for the $\Delta H°$ values.[23]

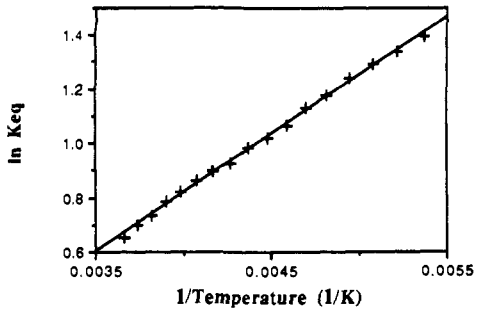

Figure 10. van't Hoff plot for non-hydrogen-bonded vs intramolecularly hydrogen-bonded **4**, from amide proton NMR data obtained with 1 mM samples in CD_2Cl_2 at 185–275 K (Figure 9). $K_{eq} = (\delta_{obsd} - \delta_n)/(\delta_b - \delta_{obsd})$, where δ_{obsd} is the chemical shift of the amide proton of **4** at that temperature, δ_n is the chemical shift of the amide proton of **15** at that temperature, and δ_b is given by the $\Delta\delta/\Delta T$ function passing through 8.40 ppm at 295 K with a slope of -5.0×10^{-3} ppm/K (ref 1). The line represents the best fit to the equation $\ln K_{eq} = -\Delta H°/RT + \Delta S°/R$, with $\Delta H° = -0.9$ kcal/mol and $\Delta S° = -1.8$ eu (correlation coefficient = 0.998).

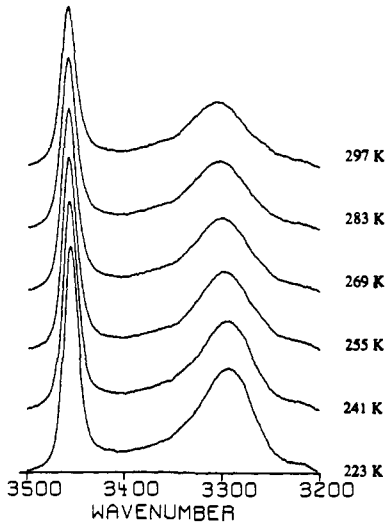

Figure 11. NH stretch region of FT-IR spectral data for 1 mM diamide **5** in CH_2Cl_2, as a function of temperature, after subtraction of the spectrum of pure CH_2Cl_2 at the same temperature. Absorption maxima at 297 K: 3459 (non-hydrogen-bonded) and 3306 cm^{-1} (intramolecularly hydrogen-bonded).

Figure 11 shows variable-temperature IR data from the NH stretch region obtained for a 1 mM solution of diamide **5** in CH_2Cl_2 at 223–297 K. The spectrum at the highest temperature is similar to that for flexible diamide **2** under identical conditions,[1] showing a major band at 3459 cm^{-1}, for a solvated NH moiety, and a smaller band at 3306 cm^{-1}, for an intramolecularly hydrogen-bonded NH moiety. The non-hydrogen-bonded band remains dominant for **5** throughout the temperature range examined.

Figure 12 shows $\Delta\delta NH/\Delta T$ data for **5** and **2**. For **5**, the variation of δNH with temperature is not monotonic, which is extremely unusual in our experience. These data suggest that the extent of intramolecular hydrogen bonding is similar for **5** and

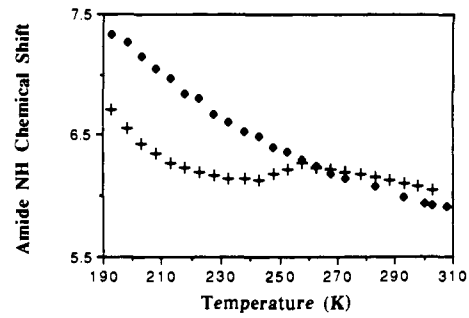

Figure 12. Amide proton NMR chemical shifts, for 1 mM solutions in CD_2Cl_2, as a function of temperature: diamide **5** (+); diamide **2** (◆) (ref 1).

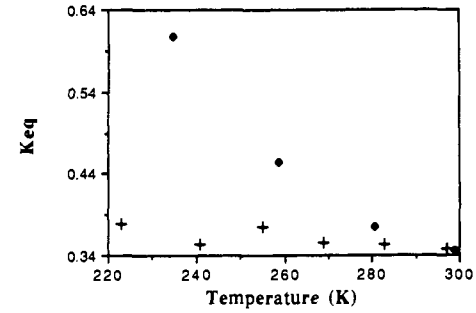

Figure 13. IR-based equilibrium constants for non-hydrogen bonded vs intramolecularly hydrogen-bonded states of diamide **5** (+) and diamide **2** (◆) as a function of temperature in CH_2Cl_2. These values were calculated from NH stretch region IR data for 1 mM samples of the diamides, using data from a 1 mM sample of *N*-methylacetamide to determine the integrated extinction coefficient of the non-hydrogen-bonded NH stretch band.

2 in the range 300–260 K, slowly increasing with decreasing temperature. Between 260 and 240 K, however, δNH of **5** shows an inverse temperature dependence, relative to **2**. The data in Figure 12 suggest that **5** experiences a smaller extent of intramolecular hydrogen bonding than does the more flexible diamide **2** at all temperatures below 260 K.

The nonmonotonic relationship between temperature and the extent of intramolecular hydrogen bonding in **5** is also evident from analysis of the IR data. Figure 13 shows the population of intramolecularly hydrogen-bonded forms of **5** and **2** in CH_2Cl_2, as a function of temperature; the populations were calculated from the data in Figure 11 and analogous data for **2**[1] by using variable-temperature IR data from a 1 mM solution of *N*-methylacetamide to determine the temperature dependence of the integrated absorption of the non-hydrogen-bonded NH stretch. Flexible diamide **2** shows a monotonic increase in the intramolecularly hydrogen-bonded population as the temperature is lowered, but diamide **5** does not. The complex behavior of **5** manifested in Figures 12 and 13 suggests that a simple two-state model does not apply, and van't Hoff analysis was not undertaken.

IR Data for Diamides 6–9. Figure 14 shows the NH stretch region IR data for 1 mM samples of diamides **6–9** in CH_2Cl_2 at room temperature. Also shown, for comparison, is a spectrum of diamide **2** and a spectrum of olefinic amide **26** obtained under the same conditions. These data indicate that the extent of

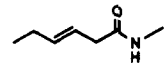

26

intramolecular C=O···H—N hydrogen bonding increases steadily across the series **6–8**; the extent of intramolecular C=O···H—N hydrogen bonding in *cis*-diamide **9** appears to be intermediate between the extents in **6** and **7**. The data also indicate that the behavior of these olefinic diamides does not conform to a simple two-state model, non-hydrogen-bonded vs intramolecularly hydrogen-bonded, because the spectra in Figure 14a–d show evidence of at least three NH stretch bands. In all cases, there is an NH

(23) As a further check on the reproducibility of the NMR-based thermodynamic analyses, we carried out an analysis of **3** using the $\Delta\delta NH/\Delta T$ data for **15** (instead of the data for the 1:1 mixture of *N*-methylacetamide and *N*,*N*-dimethylacetamide) to model the non-hydrogen-bonded state. This analysis indicated the intramolecularly hydrogen-bonded state of **3** to be enthalpically favored by 1.3 kcal/mol and entropically disfavored by 3.2 eu, in methylene chloride. Reanalysis of **4** using the $\Delta\delta NH/\Delta T$ data for the monoamide mixture (instead of **15**) to model the non-hydrogen-bonded state indicated the intramolecularly hydrogen-bonded state to be enthalpically favored by 0.9 kcal/mol and entropically disfavored by 2.0 eu. The agreement of these $\Delta H°$ and $\Delta S°$ values with the values determined for **3** and **4** by other NMR- and IR-based analyses provides an additional indication of the accuracy of these thermodynamic parameters.

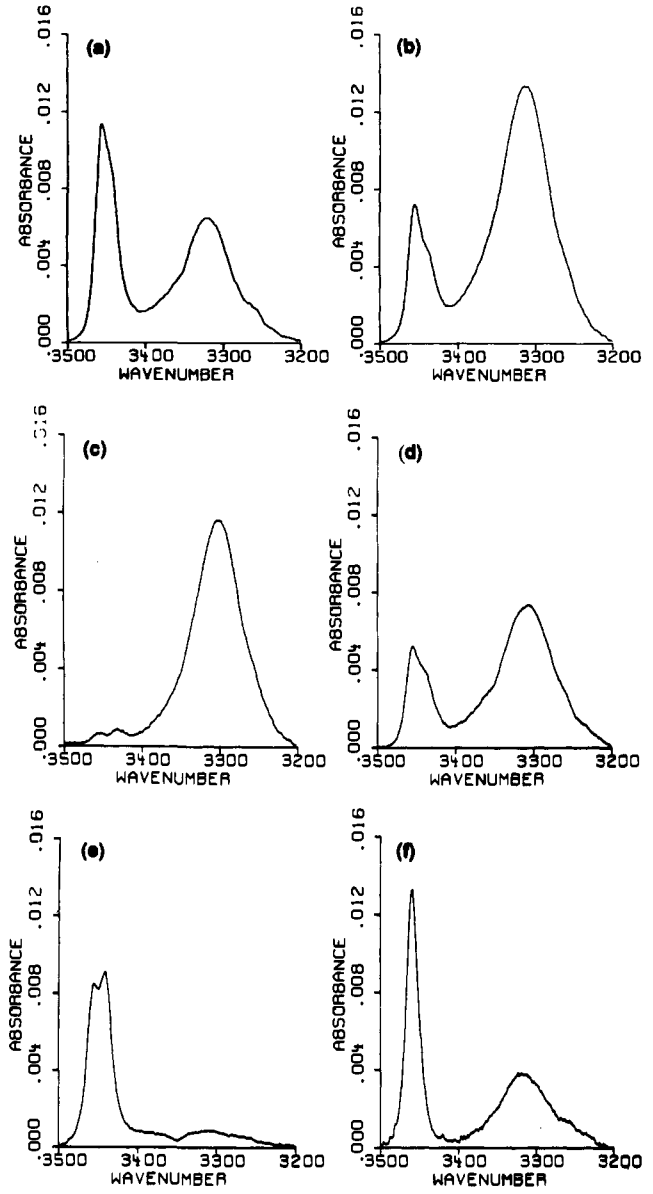

Figure 14. NH stretch region of FT-IR spectral data for 1 mM amide samples in CH_2Cl_2 at 297 K, after subtraction of the spectrum of pure CH_2Cl_2 at the same temperature: (a) diamide **6** (maxima at 3453 and 3315 cm^{-1}); (b) diamide **7** (maxima at 3453 and 3313 cm^{-1}); (c) diamide **8** (absorption maxima at 3455, 3430, and 3301 cm^{-1}); (d) diamide **9** (maxima at 3450 and 3301 cm^{-1}); (e) amide **26** (maxima at 3455 and 3442 cm^{-1}); and (f) diamide **2** (maxima at 3451 and 3317 cm^{-1}).

stretch band at ca. 3440 cm^{-1} (appearing as a shoulder on the highest energy band in Figure 14a,b,d), which we assign to an amide proton hydrogen-bonded intramolecularly to the olefin π system. Evidence for this assignment may be found in the spectrum of olefinic amide **26** in CH_2Cl_2 (Figure 14e), which shows partially resolved bands at 3455 and 3442 cm^{-1}. Diamide **2**, on the other hand, shows only one narrow band above 3400 cm^{-1} (Figure 14f).

Figure 15 shows the NH stretch region IR data for 10 mM samples of **6–9** in CH_3CN at room temperature. Diamide **6** appears not to experience any intramolecular hydrogen bonding in this moderately interactive solvent: Figure 15a shows only a band at 3401 cm^{-1}, which is indicative of an amide NH hydrogen bonded to a solvent nitrile group.[1] Diamide **7**, on the other hand, experiences a substantial amount of intramolecular C=O···H—N hydrogen bonding, as indicated by the band at 3309 cm^{-1}. Diamide **8** is predominantly intramolecularly hydrogen bonded, and diamide **9** appears to have a minor population of internally hydrogen-bonded states.[24]

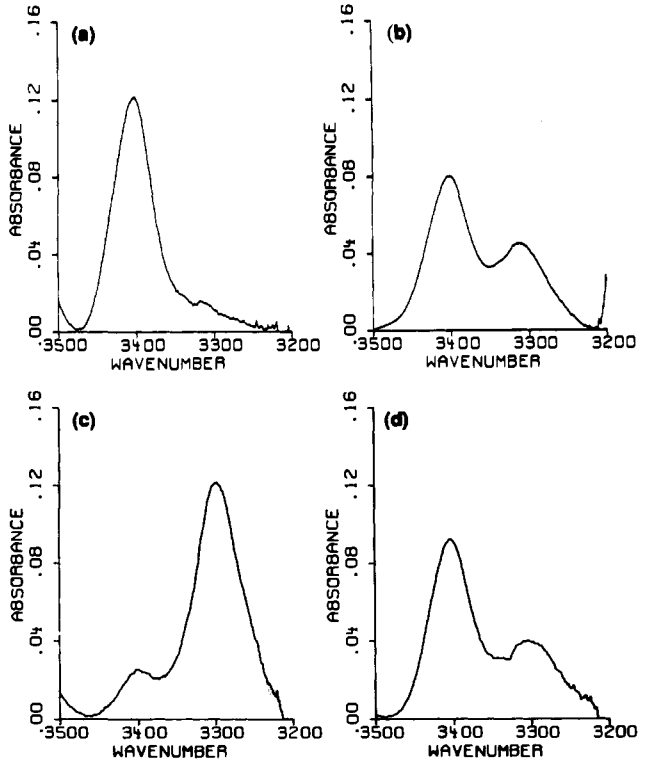

Figure 15. NH stretch region of FT-IR spectral data for 10 mM amide samples in CH_3CN at 297 K, after subtraction of the spectrum of pure CH_3CN at the same temperature: (a) diamide **6** (maximum at 3401 cm^{-1}); (b) diamide **7** (maxima at 3401 and 3309 cm^{-1}); (c) diamide **8** (maxima at 3401 and 3300 cm^{-1}); and (d) diamide **9** (maxima at 3403 and 3304 cm^{-1}).

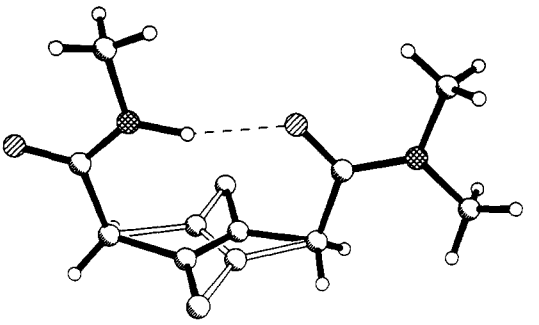

Figure 16. Ball-and-stick representation of diamide **8** in the crystalline state. The intramolecular N—H···O=C hydrogen bond is indicated by the dotted line. Disorder in the olefinic portion of the structure could be modeled as an approximately 1:1 mixture of the two conformations shown.

Crystal Structures of 8 and a Derivative of 6. Efforts to grow crystals suitable for diffraction were successful for diamides **8** and **27**, the latter an adamantyl derivative of **6**. (In a related system,

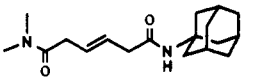

27

we have shown that this type of terminal adamantyl substitution does not disrupt nine-membered-ring N—H···O=C hydrogen bonding in solution or the solid state.[25]) As shown in Figure 16, **8** contains an intramolecular hydrogen bond in the solid state, with what appears to be an excellent geometry: O···H distance, 1.94

(24) IR data for 10 mM solutions of **3** and **4** in CH_3CN show that these diamides have detectable but small populations of C=O···H—N hydrogen-bonded conformations in this solvent. In both cases, the population of intramolecularly hydrogen-bonded states appears to be smaller than is observed for **9**.

(25) Dado, G. P.; Desper, J. M.; Holmgren, S. K.; Rito, C. J.; Gellman, S. H. *J. Am. Chem. Soc.* **1992**, *114*, 4834.

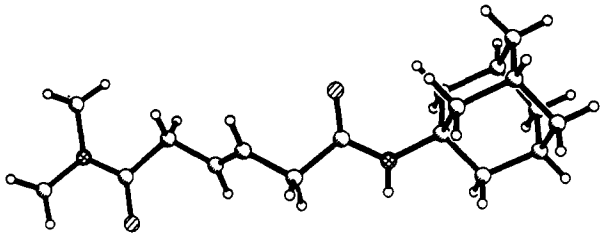

Figure 17. Ball-and-stick representation of diamide **27** in the crystalline state. The intermolecular hydrogen bonds are not shown.

(5) Å; N—H···O angle, 164 (4)°; C=O···H angle, 130 (1)°; and N—C=O···H torsion angle, 8 (4)° (the last value indicates little out-of-plane distortion; the hydrogen-bonded hydrogen atom was independently refined). Disorder in the olefinic carbons could be modeled as an approximately 1:1 mixture of the two orientations shown in Figure 16. Figure 17 shows that **27** adopts an extended conformation in the solid state, experiencing only intermolecular hydrogen bonding. The amide hydrogen atom was not independently refined in this case. The O···H distance seems to be long, ca. 2.34 Å, but the angular relationships appear to fall in normal ranges (N—H···O angle ca. 171°, C=O···H angle ca. 140°, and N—C=O···H torsion angle ca. 19°).

Discussion

Comparison of ^{1}H NMR-Derived and IR-Derived Thermodynamic Data. The two states for each diamide, intramolecularly hydrogen-bonded and non-hydrogen-bonded,[3] probably each comprise multiple conformations. Interpretation of the NMR data is further complicated by the fact that the observed resonances are weighted averages of the contributions from the non-hydrogen-bonded and intramolecularly hydrogen-bonded states. The reasonably good quantitative agreement between ^{1}H NMR-based and IR-based thermodynanic analyses of hydrogen-bonding equilibria for **3** and **4** (and the agreement previously observed for **2**[1]) suggests that these two spectroscopic methods are similarly sensitive to the difference between "hydrogen-bonded" and "non-hydrogen bonded"[3] states. Thus, these operationally defined states have a physical significance that transcends the method used to detect them. (We do not believe that an attempt to interpret the small differences between NMR- and IR-derived $\Delta H°$ and $\Delta S°$ values would be warranted, particularly in light of the assumptions required for the NMR-based approach.)

Rigidification of the Three-Carbon Linker. The results of the molecular mechanics conformational searches were consistent with the chemist's intuitive sense that flexible diamides **1** and **2** can accommodate the intramolecular hydrogen bond in several different backbone conformations. Because the accuracy with which such calculations identify favorable folding patterns of small amides is unclear,[26] we treated these computational results as only qualitatively suggestive of rigidification strategies.

In methylene chloride, the intramolecularly hydrogen-bonded state of **3** is significantly more favorable enthalpically than the non-hydrogen-bonded state, which contrasts with the enthalpic similarity of these two states for **1**. The variation in $\Delta H°$ values does not arise exclusively from differences in intramolecular hydrogen bond strength, but reflects instead the combined effects of hydrogen bond energy, torsional strain, nonbonded repulsions, and perhaps other interactions present in the intramolecularly hydrogen-bonded state but not in the non-hydrogen-bonded state (or vice versa). The difference in $\Delta H°$ between **1** and **3** is consistent with the MM2 suggestion that formation of a geometrically optimal N—H···O=C interaction by **1** (in vacuo) requires at least one nearly eclipsed CH_2—CH_2 bond. Since eclipsing interactions are unavoidable in cyclopentane rings,[12] the enthalpic gain associated with hydrogen bond formation in **3** in the nonpolar solvent should not be opposed by developing torsional strain. For **1**, on the other hand, eclipsing interactions that accompany hydrogen bond formation will affect the enthalpy difference between the non-hydrogen-bonded and intramolecularly hydrogen-bonded states, because the lowest energy non-hydrogen-bonded conformation is presumably completely extended and lacks torsional strain.

If optimal hydrogen-bond geometry in **1** does indeed require eclipsing interactions, then one might expect the low level of intramolecular hydrogen bonding occurring in **1** to involve N—H···O=C interactions of poor geometry. Nonoptimal hydrogen bond geometry in **1** could explain the observation that, despite the diminished flexibility of **3** relative to **1**, adoption of the intramolecularly hydrogen-bonded state involves similar entropic costs in both cases, with $\Delta S°$ perhaps slightly less unfavorable for the more flexible diamide. Optimal hydrogen-bonding geometries are more spatially restrictive than nonoptimal geometries;[27] for example, the region of space around the acceptor oxygen atom that allows an N—H···O angle of 170° is smaller than the region that allows 150°. Thus, formation of an enthalpically more favorable intramolecular hydrogen bond is likely to involve a larger penalty in conformational entropy. (Enthalpy/entropy compensation is often observed in processes controlled by networks of noncovalent interactions, and several origins of this compensation have been proposed;[28] the relationship between the enthalpic gain and entropic cost associated with hydrogen-bond formation is one possible source of this compensation.) The similarity of the entropic costs for hydrogen-bonded ring closure of **1** and **3** could also indicate that the 1,3-cyclopentyl linker reduces the conformational freedom of the intramolecularly hydrogen-bonded and non-hydrogen-bonded states to similar extents, relative to the more flexible linker.

Intramolecular hydrogen bond formation in spiro lactam **4** appears to be slightly less entropically costly than in **3**, a result that is consistent with our expectation that the additional constraint of **4** would eliminate more non-hydrogen-bonded conformations than intramolecularly hydrogen-bonded conformations. The incorporation of the lactam ring also diminishes the enthalpic stabilization of the internally hydrogen-bonded state, which was not anticipated. One possible explanation for this enthalpic effect is that the lactam carbonyl of **4** is an intrinsically poorer hydrogen bond acceptor than the acyclic tertiary amide group of **3**. The amide I bands (predominantly C=O stretch) of small-ring lactams typically occur at higher energy than those of analogous acyclic amides. Thus, the lactam amide I band of **15** (no possible intramolecular hydrogen bonding) occurs at 1676 cm^{-1}, while the amide I band of *N,N*-dimethylacetamide occurs at 1652 cm^{-1}. The higher energy of the lactam amide I band is conventionally interpreted to reflect a higher C=O bond order and a corresponding decrease in electron density at the oxygen atom, which should diminish the hydrogen-bonding-acceptor ability of the lactam carbonyl relative to an acyclic amide carbonyl.

The $\Delta S°$ values for hydrogen-bonded ring closure in **1**, **3**, and **4** in methylene chloride are all low in comparison to the entropic cost of ring closure by covalent bonds.[29] In discussing the similar situation for **2**, we previously suggested several possible explanations for the seemingly small $\Delta S°$ value, including solvation effects and residual entropy in the low-lying vibrationally excited states of the hydrogen bond.[1] Doig and Williams have recently noted a related effect in their reanalysis of data on intermolecularly hydrogen-bonded systems.[30] Formation of intermolecularly

(26) (a) Gellman, S. H.; Dado, G. P. *Tetrahedron Lett.* **1991**, *32*, 7377. (b) Dado, G. P.; Gellman, S. H. *J. Am. Chem. Soc.* **1992**, *114*, 3138 and references therein. (c) McDonald, D. Q.; Still, W. C. *Tetrahedron Lett.* **1992**, *33*, 7743 and 7747.

(27) (a) Pedersen, B. *Acta Crystallogr.* **1974**, *B30*, 289. (b) Kroon, J.; Kanters, J. A.; van Duijneveldt-van de Rejdt, J. G. C. M.; van Duijneveldt, F. B.; Vliegenthart, J. A. *J. Mol. Struct.* **1975**, *24*, 109. (c) Olovsson, I.; Jönsson, P.-G.; In *The Hydrogen Bond*; Schuster, P., Zundel, G., Sandorfy, C., Eds.; North-Holland: Amsterdam, 1976; Vol. 2, pp 393–456.

(28) Lumry, R. In *Bioenergetics and Thermodynamics*; Braibanti, A., Ed.; D. Reidel Publishing Company, Dordrecht, The Netherlands, 1980; pp 405–423 and references therein.

(29) Page, M. I.; Jencks, W. P. *Proc. Natl. Acad. Sci. U.S.A.* **1971**, *68*, 1678.

(30) Doig, A. J.; Williams, D. H. *J. Am. Chem. Soc.* **1992**, *114*, 338. The views expressed in this article have recently been modified; see: Williams, D. H. Aldrichimica *Acta* **1992**, *25*, 9.

hydrogen-bonded dimers (e.g., of valerolactoam) in nonpolar solvents appears to have a lower entropic cost than might be expected for a process that converts two independent particles to one, which led Doig and Williams to conclude that hydrogen bond formation in solution is "entropy driven". While Doig and Williams' observations on the entropy of hydrogen-bond-mediated dimerization are consistent with our prior findings in the intramolecular regime, it should be pointed out that neither set of results implies that hydrogen bond formation is "entropy driven". The dimerization-promoting ΔS_{hbond} (>0) that was formally derived by Doig and Williams stemmed from their assumption that the molecules associated in the dimer are rigidly held relative to one another. This assumption is unrealistic, because the attractive potential of the hydrogen bonds is much "shallower" than that of a covalent bond.[31] Thus, Doig and Williams' ΔS_{hbond} probably represents degrees of monomer translational and rotational freedom that are converted to vibrational freedom in the loose, hydrogen-bonded dimer, rather than a fundamentally new contribution of the hydrogen bonds to the dimer's total entropy.

Rigidification of the Four-Carbon Linker. The intramolecular hydrogen bond of diamide **3** involves a nine- as well as an eight-membered ring. The *cis*-1,3-disubstituted cyclopentane skeleton may be viewed as constraining the four-carbon linker such that the central and at least one other CH_2–CH_2 bond adopt gauche torsion angles. If such a backbone conformation characterized the most favorable intramolecularly hydrogen-bonded state of **2**, then one would expect $\Delta H°$ to be more favorable for **3** (in which the torsional strain cost has been "prepaid" in the rigidification process) than for **2**. In fact, as indicated in Table I, the enthalpic differences between these two states are very similar for **2** and **3**. This similarity in $\Delta H°$ suggests that **2** may have intramolecularly hydrogen-bonded conformations available to it that involve fewer enthalpic penalties than does the nine-membered-ring conformation required by the rigidified backbone of **3**. It is also possible, however, that unfavorable steric interactions involving the "extra" methylene in **3** relative to **2** create enthalpic opposition to internal hydrogen bond formation in **3** that is not found in **2**.

Diamide **5** represents an attempt to constrain only the central CH_2—CH_2 bond in the nine-membered hydrogen-bonded ring. It is clear that this rigidified backbone does not promote an intramolecular N—H···O=C interaction relative to the flexible backbone of **2** (Figures 12 and 13). This comparison suggests that the most favorable intramolecularly hydrogen-bonded conformation of **2** does not involve a gauche torsion angle at the central CH_2—CH_2 bond. It is also possible that unfavorable steric interactions between the substituents bearing the amide groups and the cyclohexyl ring (interactions that could not occur in **2**) are deleterious to hydrogen-bond formation in **5**.

The IR data for olefinic diamides **6–9** in CH_2Cl_2 (Figure 14) show that the extent of intramolecular N—H···O=C hydrogen bonding increases dramatically as methyl groups are added to the alkene carbons. Although N—H···π hydrogen bonds also occur in these molecules, this weaker interaction probably does not provide a significant conformation-directing force, as judged by comparisons among **2**, **6**, and **8**: the extent of intramolecular hydrogen bonding is similar in **2** (no double bond) and **6** (double bond but no methyl groups), both of which experience considerably less hydrogen bonding than **8** (two methyl groups on the double bond). The promotion of intramolecular N—H···O=C hydrogen bond formation by the rigidified linking segments of **7–9** is so effective that the interaction is detectable in acetonitrile, a solvent that is considerably more polar than methylene chloride. We have previously shown that little or no intramolecular hydrogen bonding occurs in acetonitrile solutions of **1** or **2**,[1] apparently because of intermolecular hydrogen-bonding competition from the solvent. Figure 15a shows that **6** also experiences little or no N—H···O=C hydrogen bonding under these conditions. Both **7** and **9**, however, have minor but significant populations of N—H···O=C hydrogen-bonded conformations, and intramolecular N—H···O=C hydrogen bonding predominates for **8**. The behavior of **6–9** is consistent with the hypothesis that geminal and cis substituents on the double bonds encourage the amide groups to reside above or below the plane of the C—C=C—C unit, increasing the likelihood that the amide groups will be near one another. This type of conformation-directing effect involves allylic 1,2- and 1,3-strain, as identified by Johnson,[15] and similar effects have been invoked to explain reaction selectivity in a number of cases.[14] The crystal structure of **8** shows that the *trans*-olefin-containing linker allows formation of a nine-membered-ring N—H···O=C hydrogen bond of good geometry. This structural information suggests that a conformation of **2** containing the sequence g^+ag^- about the three CH_2—CH_2 bonds could also accommodate a hydrogen bond of good geometry.

Our observations with **6–9** may be relevant to the design of "peptidomimetic" units, molecular fragments that can replace two or more amino acid residues in peptides or proteins.[32] Medicinal chemists often seek isosteric but hydrolytically inert replacements for the secondary amide moieties found in the backbones of natural peptides. The *trans*-alkene unit has received considerable attention in this context.[33] The trend in behavior among **6–8** suggests that methyl-substituted *trans*-alkene units may be fruitful choices if the peptide unit to be replaced occurs in a segment that must adopt a folded conformation for proper function (e.g., between residues $i + 1$ and $i + 2$ of a β-turn[6a]).

More generally, our findings show that the use of intramolecular hydrogen-bond formation for the detection of folded states allows one to identify frameworks with high propensities to adopt compact conformations (e.g., the skeletons of **3** and **8**). These types of structural units should prove useful in the development of semi-proteins[34] and new polymers[4] with defined folding properties.

Experimental Section

General. All melting points are uncorrected. Reagents employed were either commercially available or prepared according to a known procedure. In reactions requiring anhydrous conditions, solvents were dried by distillation under N_2 from the appropriate drying agent (THF and diethyl ether, from Na^0; CH_3OH, from Mg; benzene, toluene, CH_2Cl_2, and DMF (under vacuum), from CaH_2). Glassware was either oven- or flame-dried and then cooled under a steady stream of dry N_2. For anhydrous reactions, flasks were equipped with rubber septa and maintained under a small positive N_2 pressure; reagent transfer was performed by syringe or cannula techniques. All chromatography solvents were reagent grade, except *n*-hexane and CH_2Cl_2, which were purified by flash distillation. Thin-layer chromatography was performed using silica gel 60 F-254 plates (EM). Column chromatography was carried out using low N_2 pressure with 230–400 mesh silica gel from EM Science. Columns eluted with small percentages of CH_3OH in $CHCl_3$ were slurry-packed after the slurry had been stirred with the eluant for at least an hour. Fresh solvent was then passed through the column continuously until subtle changes in the gray hue of the silica had moved completely through the column bed (for 2% (v/v) CH_3OH or less, this pre-equilibration of the column could be quite time-consuming). This pre-equilibration was essential for optimal resolution. NMR spectroscopy was performed on a Bruker WP-200 spectrometer operating at 200 MHz for routine observation of hydrogen and on a Bruker WP-270 spectrometer operating at 67.5 MHz for observation of carbon-13. Chemical shifts are reported relative to TMS (0 ppm) or relative to the isotopic impurity peak for a given solvent ($CDCl_3$, 7.26 ppm for proton and 77.0 ppm for carbon; CD_3CN, 1.95 ppm; CD_2Cl_2, 5.32 ppm). FT-IR spectra were obtained on a Mattson Polaris spectrometer (routine characterization)

(31) Muller, N.; Reiter, R. C. *J. Chem. Phys.* **1965**, *42*, 3265.

(32) Hirschmann, R. *Angew. Chem., Int. Ed. Engl.* **1991**, *30*, 1278 and references therein.

(33) (a) Hann, M. M.; Sammes, P. G.; Kennewell, P. D.; Taylor, J. B. *J. Chem. Soc., Chem. Commun.* **1980**, 234. (b) Cox, M. T.; Heaton, D. W.; Horbury, J. *J. Chem. Soc., Chem. Commun.* **1980**, 799. (c) Spaltenstein, A.; Carpino, P. A.; Miyake, F.; Hopkins, P. B. *J. Org. Chem.* **1987**, *52*, 3759. (d) Shue, Y.-K.; Carrera, G. M.; Tufano, M. D.; Nadzan, A. M. *J. Org. Chem.* **1991**, *56*, 2107. (e) Ibuka, T.; Habashita, H.; Otaka, A.; Fujii, N.; Oguchi, Y.; Uyehara, T.; Yamamoto, Y. *J. Org. Chem.* **1991**, *56*, 4370. (f) Bol, K. M.; Liskamp, R. M. J. *Tetrahedron Lett.* **1991**, *32*, 5401.

(34) For leading references on the use of rigidified templates to stabilize secondary structure and tertiary structure in peptides, see: (a) Kemp, D. S. *Trends Biotechnol.* **1990**, *6*, 246. (b) Kemp, D. S.; Boyd, J. G.; Mundel, C. *Nature* **1991**, *352*, 451. (c) Mutter, M.; Vuilleumier, S. *Angew. Chem., Int. Ed. Engl.* **1989**, *28*, 535.

or on a Nicolet 740 spectrometer. High-resolution electron impact ionization mass spectroscopy was performed on a Kratos MS-25 spectrometer.

Variable-Temperature Spectroscopic Experiments. Substrates and solutions were prepared as previously described.[1] The purity of amide samples used for spectroscopic analysis was evaluated by examination of the 500-MHz ^{1}H NMR spectra; all samples were judged to be ≥95% pure. In particular, only a single amide proton resonance could be detected in each case. Variable-temperature ^{1}H NMR experiments were performed on a Bruker AM-500 spectrometer as previously described.[1]

For quantitative analysis of IR spectra, the concentration of non-hydrogen-bonded conformers in a CH_2Cl_2 solution was determined from the integrated absorbance of the non-hydrogen-bonded amide NH stretch band (absorption maximum usually 3450–3460 cm^{-1}; integration window 3400–3500 cm^{-1}), using a normalized integrated absorbance that had been obtained from the same type of measurement with an appropriate model compound. First-order base line corrections were applied to obtain the spectra reproduced in the figures, but base line corrections were not applied when absorption bands were integrated.

IR measurements were performed on a Nicolet 740 FT-IR spectrometer equipped with a TGS detector. A Specac vacuum-tight variable-temperature cell P/N 21500 equipped with CaF_2 crystal windows and having a path length of 1 mm was used for variable-temperature experiments. Because the cell path length is determined by the thickness of the soft lead spacer between the two CaF_2 crystals, the cell path length could slowly diminish over time. All quantitative IR measurements were carried out with the same cell over a short period of time, so that variations in the absolute path length would not effect the analysis.

Temperatures were maintained with various ice, dry ice, and liquid N_2 slush baths and were monitored with a platinum resistance thermometer attached directly to the CaF_2 crystal window. The cell temperature was allowed to stabilize for at least 20 min before a measurement was obtained, and the cell temperature varied less than 1.5 °C during data acquisition. Spectra of 128 scans were obtained with 2 cm^{-1} resolution. Solvent subtraction was carried out using reference spectra obtained at the same temperatures as the sample spectra.

***cis*-3-(*N*,*N*-Dimethylcarbamoyl)cyclopentane-1-carboxylic Acid (11).** Cyclopentane-*cis*-1,3-dicarboxylic acid anhydride **10**[16] (0.25 g, 1.8 mmol) was dissolved in 2 mL of 20% (w/w) aqueous $(CH_3)_2NH$ with stirring at room temperature. After 1 h, the reaction solution was cooled to 0 °C and carefully acidified with concentrated HCl. The acidified mixture was extracted several times with $CHCl_3$. The extracts were combined, washed with brine, dried with $MgSO_4$, filtered, and evaporated to yield 0.32 g (95%) of **11** as a white crystalline solid: mp 119–120 °C; ^{1}H NMR ($CDCl_3$, ppm) 1.87–2.24 (m, 6 H, 3 × CH_2), 2.99 (s, 3 H, NCH_3), 3.0 (m, 1 H, $CHCO_2$), 3.11 (s, 3 H, NCH_3), 3.24 (m, 1 H, CHCO), 8.5 (s, very broad, 1 H, CO_2H); ^{13}C NMR ($CDCl_3$, ppm) 29.97 (CH_2), 31.19 (CH_2), 32.09 (CH_2), 36.05 (CH_3), 37.51 (CH_3), 41.55 (CH), 44.81 (CH), 176.80 (C=O), 178.16 (C=O); IR (KBr, cm^{-1}) 893, 1164, 1203, 1608, 1724, 2980 (very broad); MS (EI, *m/e*) 185.1056 (calcd for $C_9H_{15}NO_3$ 185.1052).

***N*,*N*,*N*'-Trimethylcyclopentane-*cis*-1,3-dicarboxamide (3).** A solution of **11** (0.5 g, 2.7 mmol) in anhydrous THF (20 mL) was treated with *N*-hydroxysuccinimide (0.47 g, 4.0 mmol) and dicyclohexylcarbodiimide (0.7 g, 3.5 mmol). A white precipitate soon formed. The resulting mixture was stirred under N_2 at room temperature for 2 h. After the reaction mixture was cooled to 0 °C, CH_3NH_2 was bubbled through for 10–15 min. The resulting slurry was stirred at 0 °C for 20 min and room temperature for 17 h. The precipitated solid was removed by filtration and washed with CH_2Cl_2. The combined filtrate was concentrated, and the residue was purified by silica column chromatography eluting with 5–10% (v/v) CH_3OH in $CHCl_3$ to yield 400 mg (75%) of **3** as a viscous oil that solidified upon standing: mp 60–62 °C; ^{1}H NMR ($CDCl_3$, ppm) 1.7–2.2 (m, 6 H, 3 × CH_2), 2.72 (d, J = 4.8 Hz, 3 H, NCH_3), 2.73 (m, 1 H, CHCO), 2.90 (s, 3 H, NCH_3), 3.02 (s, 3 H, NCH_3), 3.03 (m, 1 H, CHCO), 7.73 (broad, 1 H, CONH); ^{13}C NMR ($CDCl_3$, ppm) 26.13 (CH_3), 30.72 (CH_2), 31.84 (CH_2), 32.28 (CH_2), 35.79 (CH_3), 37.35 (CH_3), 40.80 (CH), 46.82 (CH), 176.45 (C=O), 176.85 (C=O); IR (1 mM in CH_2Cl_2, cm^{-1}) 1621, 1639, 1659 (shoulder), 2949, 3292, 3459; ME (EI, *m/e*) 198.1368 (calcd for $C_{10}H_{18}N_2O_2$ 198.1368).

***cis*-*N*-Methyl-3-(methoxycarbonyl)spiro[cyclopentane-1,3'-pyrrolidin]-2'-one (13) and *trans*-*N*-Methyl-3-(methoxycarbonyl)spiro[cyclopentane-1,3'-pyrrolidin]-2'-one (14).** *n*-Butyllithium (23 mL, 2.5 M in hexane, 57.5 mmol) was added dropwise under N_2 to a stirred solution, cooled to −5 °C, of diisopropylamine (8.4 mL, 60 mmol) in anhydrous THF (200 mL). After being stirred for another 15 min at 0 °C, the solution was cooled to −78 °C and a solution of dimethyl cyclopentane-1,3-dicarboxylate[17] (9.0 g, 48 mmol) in anhydrous THF (25 mL) was added dropwise through a cannula. The resulting yellow mixture was stirred at −78 °C for another 30 min. Allyl bromide (4.7 mL, 54 mmol), passed through a short alumina column immediately before use, was added in one portion. The cooling bath was then removed, and the mixture was allowed to warm to room temperature over a period of 1.5 h. The reaction was quenched by adding saturated aqueous NH_4Cl (50 mL). The aqueous mixture was extracted with diethyl ether. The ether extracts were combined, washed with brine, dried with $MgSO_4$, and concentrated. The liquid residue was purified by silica column chromatography eluting with 20% (v/v) ethyl acetate in *n*-hexane, yielding 8.5 g (78%) of dimethyl 1-allylcyclopentane-1,3-dicarboxylate, as a diastereomeric mixture, as a slightly yellow liquid: ^{1}H NMR ($CDCl_3$, ppm) 1.5–2.5 (m, 8 H, 4 × CH_2), 2.84 (m, 1 H, CH), 3.66 (s, 6 H, 2 × CH_3), 5.0 (m, 2 H, =CH_2), 5.6 (m, 1 H, =CH); ^{13}C NMR ($CDCl_3$, ppm) 28.57 and 34.06 (CH_2), 34.79 and 35.10 (CH_2), 38.08 and 38.49 (CH_2), 42.79 and 42.87 (CH), 43.87 and 44.21 (CH_2), 51.61 and 51.75 (CH_3), 53.33 and 53.68 (C), 117.74 and 117.87 (=CH_2), 134.08 (H-C=), 175.62, 176.10, 176.63, and 176.77 (2 × C=O); IR (neat, cm^{-1}) 920, 1172, 1207, 1436, 1641, 1732, 2953, 3078; MS (EI, *m/z*) 226.1210 (calcd for $C_{12}H_{18}O_4$ 226.1205).

A 250-mL three-necked rounded-bottomed flask, fitted with a gas inlet and an outlet with drying tube, was charged with the diastereomeric mixture of dimethyl 1-allylcyclopentane-1,3-dicarboxylate (2.0 g, 8.85 mmol), distilled CH_2Cl_2 (100 mL), and a magnetic stir bar. The reaction solution was cooled to −78 °C, and O_3 was bubbled into the solution until a light blue color persisted. The excess O_3 was then purged from the reaction with N_2 until the blue color disappeared. $(CH_3)_2S$ (2 mL, 26.6 mmol) was added and the cooling bath was then removed. The reaction mixture was allowed to warm to room temperature slowly. The mixture was treated then with zinc dust (1.0 g, 15 mmol), and acetic acid was added slowly into the stirred zinc slurry over a period of 30 min. The mixture was filtered, and the filtrate was poured into saturated aqueous $NaHCO_3$ (100 mL). The organic layer was separated, and the aqueous layer was extracted with two 50-mL portions of CH_2Cl_2. The combined organic solutions were washed with brine, dried with $MgSO_4$, and concentrated to yield 2.1 g (quantitative crude yield) of a diastereomeric mixture of dimethyl 1-(formylmethyl)cyclopentane-1,3-dicarboxylate as a yellow oil: ^{1}H NMR ($CDCl_3$, ppm) 1.5–2.5 (m, 6 H), 2.7–3.1 (m, 3 H), 3.66–3.68 (four s, 6 H), 9.7 (two t, J = 1.1 Hz, 1 H). This crude aldehyde was carried on to the next step without further purification or characterization.

CH_3NH_2·HCl (3.0 g, 44 mmol) was dissolved in CH_3OH (40 mL), and KOH (1.2 g, 20 mmol) was added. The KOH pellets completely dissolved, and a cloudy suspension formed. The crude aldehyde (2.0 g) was added, and the mixture was stirred at room temperature for 15 min. $NaB(CN)H_3$ (330 mg, 5.0 mmol) was then added, and the mixture was stirred for 5 h. Concentrated HCl was then added to destroy any excess $NaB(CN)H_3$ (Caution: HCN gas evolved). After the mixture had stirred at pH < 2 for 2 h, KOH was added to pH ~10. The mixture was filtered, and the filtrate was extracted with four 40-mL portions of ethyl acetate. The combined organic layers were washed with brine, dried with Na_2SO_4, and evaporated under reduced pressure. The residue was further dried on a vacuum line for several hours to yield 1.4 g (65%) of a diastereomeric mixture of dimethyl 1-[2-(*N*-methylamino)ethyl]-cyclopentane-1,3-dicarboxylate as a yellow viscous oil, which was contaminated with the cyclized spiro lactam: ^{1}H NMR ($CDCl_3$, ppm) 1.6–2.5 (m, 8 H, 4 × CH_2), 2.82 and 2.83 (two d, 3 H, NCH_3), 3.1 (m, 1 H, CH), 3.25 (t, J = 6.8 Hz, 2 H, CH_2), 3.65 (two s, 6 H, 2 × NCH_3). This crude mixture was carried on to the next step without further purification or characterization.

A solution of the crude product described above (1.4 g) and isopropylamine (2.5 mL, 30 mmol) in 50 mL of absolute CH_3OH was refluxed under N_2 for 8 h. After cooling, the solvent was removed in vacuo. The residue (1.13 g, a mixture of cis and trans isomers) were separated by silica gel column chromatography eluting with 5% (v/v) CH_3OH in $CHCl_3$; the cis isomer **13** (460 mg, 24% from dimethyl 1-allylcyclopentane-1,3-dicarboxylate) was obtained as colorless liquid: ^{1}H NMR ($CDCl_3$, ppm) 1.5–2.4 (m, 8 H, 4 × CH_2), 2.84 (s, 3 H, CH_3), 3.1 (m, 1 H, CH), 3.26 (t, J = 6.8 Hz, 2 H, CH_2), 3.66 (s, 3 H, CH_3); ^{13}C NMR ($CDCl_3$, ppm) 28.10 (CH_2), 29.87 (CH_3), 33.18 (CH_2), 35.30 (CH_2), 39.62 (CH_2), 43.29 (CH), 46.26 (CH_2), 50.99 (C), 51.62 (CH_3), 175.33 (C=O), 177.65 (C=O); IR (neat, cm^{-1}) 733, 922, 1201, 1435, 1685, 1733, 2237, 2872, 2952, 3452; MS (EI, *m/z*) 211.1206 (calcd for $C_{11}H_{17}NO_3$ 211.1208). The trans isomer **14** (530 mg, 28% from dimethyl 1-allylcyclopentane-1,3-dicarboxylate) was also obtained as a colorless liquid: ^{1}H NMR ($CDCl_3$, ppm) 1.6–2.3 (m, 8 H, 4 × CH_2), 2.83 (s, 3 H, CH_3), 3.1 (m, 1 H, CH), 3.26 (t, J = 6.8 Hz, 2 H, CH_2), 3.66 (s, 6 H, 2 × CH_3); ^{13}C NMR ($CDCl_3$, ppm) 29.85 (CH_2), 29.86 (CH_3), 33.48 (CH_2), 36.29 (CH_2), 39.15 (CH_2), 43.14 (CH), 46.53 (CH_2), 50.75 (C), 51.62 (CH_3), 176.53 (C=O), 178.49 (C=O); IR (neat, cm^{-1}) 733, 922, 1202, 1435, 1685, 1732, 2238, 2870, 2952, 3447; MS (EI *m/z*) 211.1206 (calcd for $C_{11}H_{17}NO_3$ 211.1208).

***cis*-*N*-Methyl-3-(methylcarbamoyl)spiro[cyclopentane-1,3′-pyrrolidin]-2′-one (4).** A catalytic amount (~10 mg) of NaCN was added to a solution of **13** (340 mg, 1.6 mmol) in CH_3NH_2-saturated CH_3OH (12 mL). The reaction flask was tightly capped, and the solution was stirred at room temperature for 60 h. Volatiles were removed in vacuo, and the residue was taken up in $CHCl_3$, dried with $MgSO_4$, and concentrated. The crude product was purified by silica gel column chromatography, eluting with 5% (v/v) CH_3OH in $CHCl_3$ to yield 263 mg (77%) of **4** as a colorless viscous liquid: ^{1}H NMR ($CDCl_3$, ppm) 1.5–2.3 (m, 8 H, 4 × CH_2), 2.78 (d, J = 4.7 Hz, 3 H, CH_3), 2.85 (s, 1 H, CH), 2.9 (m, 1 H, CH), 3.3 (m, 2 H, CH_2), 7.8 (broad s, 1 H, NH); ^{13}C NMR ($CDCl_3$, ppm) 26.18 (CH_3), 29.97 (CH_3), 31.38 (CH_2), 34.03 (CH_2), 36.60 (CH_2), 39.26 (CH_2), 46.73 (CH), 46.97 (CH_2), 51.10 (C), 176.75 (C=O), 179.92 (C=O); IR (1 mM in CH_2Cl_2, cm^{-1}) 1653, 1670, 1681, 3290, 3458; MS (EI, m/z) 210.1369 (calcd for $C_{11}H_{18}N_2O_2$ 210.1368).

***trans*-*N*-Methyl-3-(methylcarbamoyl)spiro[cyclopentane-1,3′-pyrrolidin]-2′-one (15)** was prepared from lactam ester **14** (430 mg, 2.0 mmol) under conditions similar to those used to prepare **4** from **13**. Lactam **15** (430 mg, quantitative) was isolated as a colorless viscous liquid: ^{1}H NMR ($CDCl_3$, ppm) 1.6–2.2 (m, 8 H, cyclopentyl), 2.77 (d, J = 4.8 Hz, 3 H, NCH_3), 2.81 (s, 1 H, CH), 2.85 (m, 1 H, CH), 3.25 (t, J = 6.8 Hz, 2 H, CH_2), 6.0 (broad s, 1 H, NH); ^{13}C NMR ($CDCl_3$, ppm) 26.32 (CH_3), 29.95 (CH_3), 30.68 (CH_2), 33.72 (CH_2), 36.59 (CH_2), 40.04 (CH_2), 45.45 (CH), 46.80 (CH_2), 50.96 (C), 175.96 (C=O), 179.14 (C=O); IR (1 mM in CH_2Cl_2, cm^{-1}) 1676, 3456; MS (EI, m/z) 210.1365 (calcd for $C_{11}H_{18}N_2O_2$ 210.1368).

***N,N,N′*-Trimethylcyclohexane-*trans*-1,2-diacetamide (5).** Cyclohexane-*trans*-1,2-diacetic acid **16**[18] (0.5 g, 2.5 mmol) was refluxed in acetyl chloride (2 mL) for 1 h. Solvent was removed by distillation, and the brown solid residue was treated with 2.5 mL of 20% (w/w) aqueous $(CH_3)_2NH$. After being stirred at room temperature overnight, the reaction solution was cooled to 0 °C and acidified carefully with concentrated HCl. The acidified mixture was extracted with $CHCl_3$. The extracts were combined, dried with $MgSO_4$, filtered, and evaporated to yield 0.7 g of brown oil. The ^{1}H NMR spectrum of this material was consistent with a mixture of *trans*-2-(*N,N*-dimethylcarbamoyl)cyclohexane-1-acetic acid and *N,N,N′,N′*-tetramethylcyclohexane-*trans*-1,2-diacetamide. This crude product (0.7 g) was dissolved in 30 mL of anhydrous THF and treated with *N*-hydroxysuccinimide (0.5 g, 4 mmol) and dicyclohexylcarbodiimide (0.7 g, 3 mmol). A precipitate formed after about 15 min. The mixture was stirred under N_2 at room temperature for 2 h. The mixture was then cooled to 0 °C, and CH_3NH_2 gas was passed through for 10–15 min. The milky mixture was then stirred at 0 °C for 20 min and room temperature for 17 h. The precipitated solid was removed by filtration and washed with CH_2Cl_2. The combined filtrate was concentrated, and the residue was purified by silica gel column chromatography eluting with 5% (v/v) CH_3OH in $CHCl_3$ to yield 260 mg of **5** (35% from **16**) as a viscous oil that solidified upon standing. This material could be recrystallized from $CHCl_3$ and hexane: mp 84–86 °C; ^{1}H NMR ($CDCl_3$, ppm) 1.0–2.0 (m, 10 H, cyclohexyl), 2.0 (m, 2 H, CH_2CO), 2.6 (m, 2 H, CH_2CO), 2.78 (d, J = 4.8 Hz, 3 H, NCH_3), 2.94 (s, 3 H, NCH_3), 3.01 (s, 3 H, NCH_3), 6.27 (broad, 1 H, CONH); ^{13}C NMR ($CDCl_3$, ppm) 25.62 (CH_2), 25.76 (CH_2), 26.18 (CH_3), 32.24 (CH_2), 32.92 (CH_2), 35.53 (CH), 37.53 (CH), 37.80 (CH_2), 38.39 (CH_3), 39.48 (CH_3), 41.39 (CH_2), 172.88 (C=O), 173.32 (C=O); IR (KBr, cm^{-1}) 716, 1057, 1154, 1397, 1565, 1635, 2851, 2924, 3315; MS (EI, m/e) 240.1835 (calcd for $C_{13}H_{24}N_2O_2$ 240.1838). Also isolated was 100 mg of *N,N,N′,N′*-tetramethylcyclohexane-*trans*-1,2-diacetamide (12% from **16**) as a yellow semisolid: ^{1}H NMR ($CDCl_3$, ppm) 1.2–1.7 (m, 10 H, cyclohexyl), 2.1 (m, 2 H, CH_2CO), 2.6 (m, 2 H, CH_2CO), 2.92 (s, 6 H, 2 × CH_3), 2.99 (s, 6 H, 2 × CH_3); ^{13}C NMR ($CDCl_3$, ppm) 25.95 (CH_2), 32.96 (CH_2), 35.46 (CH), 37.53 (CH_3), 37.75 (CH_2), 39.40 (CH_3), 172.84 (C=O); IR (neat, cm^{-1}) 928, 1060, 1142, 1263, 1406, 1639, 2911, 3476; MS (EI, m/e) 254.1985 (calcd for $C_{14}H_{26}N_2O_2$ 254.1994).

***N,N,N′*-Trimethyl-3(*E*)-hexenediamide (6).** 3(*E*)-Hexenedioic acid (Aldrich, 1.0 g, 6.94 mmol) was heated at reflux in acetyl chloride (~5.0 mL) for 1 h. The solid slowly dissolved. Solvent was then removed by reduced pressure distillation. After cooling to 0 °C, the brown solid residue was treated with 20% (w/w) aqueous $(CH_3)_2NH$ (5.0 mL). All solids slowly dissolved, and the resulting brown solution was stirred at room temperature overnight. The reaction solution was washed twice with 10-mL portions of $CHCl_3$, cooled to 0 °C, acidified with concentrated HCl, and extracted three times with 30-mL portions of $CHCl_3$. These three organic extracts were combined, washed with brine, dried with $MgSO_4$, and concentrated to yield 0.34 g of 6-(*N,N*-dimethylcarbamoyl)-3(*E*)-hexenoic acid as a slightly yellow solid. A solution of this crude material (0.3 g) in 15 mL of dry THF was treated with *N*-hydroxysuccinimide (0.3 g, 2.46 mmol) and dicyclohexylcarbodiimide (0.44 g, 2.11 mmol). All solids quickly dissolved, and the resulting solution was stirred at room temperature under N_2. A white precipitate formed after about 10 min. After 90 min, the reaction mixture was cooled to 0 °C and CH_3NH_2 gas was bubbled through for 10 min. The resulting milky mixture was allowed to warm to room temperature and stirred overnight. Precipitated solids were removed by filtration and washed with $CHCl_3$. The filtrate was concentrated, and the brown reside was purified by silica gel column chromatography eluting with 5% (v/v) CH_3OH in $CHCl_3$ to yield 125 mg of **6** (39% overall) as a clear viscous oil: ^{1}H NMR ($CDCl_3$, ppm) 2.93 (s, 3 H, NCH_3), 2.94 (d, 2 H, J = 8 Hz, =$CHCH_2CO$), 3.00 (s, 3 H, NCH_3), 3.10 (d, 2 H, J = 6 Hz, CH_2), 5.60 (dt, 2 H, J = 15.5, 8 Hz, olefinic), 5.71 (dt, 2 H, J = 15.5, 6 Hz, olefinic), 6.5 (broad, 1 H, NH); ^{13}C NMR ($CDCl_3$, ppm) 26.19 (CH_3), 35.35 (CH_3), 36.70 (CH_2), 37.15 (CH_3), 39.86 (CH_2), 126.86 (CH=), 128.09 (CH=), 171.15 (C=O), 171.53 (C=O); IR (10 mM in CH_2Cl_2, cm^{-1}) 1622, 2949, 3288, 3456; MS (EI, m/z) 185.1296 (calcd for $C_9H_{16}N_2O_2$ + H 185.1290).

***N,N,N′*-Trimethyl-3(*Z*)-hexenediamide (9).** 1-Methoxy-1,4-cyclohexadiene (40 mmol) was dissolved in CH_2Cl_2 (140 mL) and CH_3OH (70 mL). One equivalent of O_3[19] was passed into the solution at −78 °C with efficient stirring. $(CH_3)_2S$ (10 mL) was then added, and the cooling bath was removed. The reaction solution was slowly warmed to room temperature under N_2 over a period of 6 h. The solvent was removed, and saturated aqueous $NaHCO_3$ (300 mL) was added to the residue. The aqueous mixture was extracted with CH_2Cl_2 (5 × 100 mL). The combined organic layers were washed with brine, dried with $MgSO_4$, and concentrated to yield 5.5 g of a yellow viscous liquid. This crude product was dissolved in acetone (300 mL), and the solution was treated with Jones reagent (5.0 g of CrO_3, 4.3 mL of concentrated H_2SO_4, and 36 mL of water) at 0 °C with stirring. The addition of the oxidant was stopped when the mixture developed a permanent orange-brown color. The mixture was stirred for another 30 min at 0 °C. Ethyl acetate (200 mL) and water (150 mL) were added followed by addition of solid Na_2SO_3 until the organic layer was clear. Acetone was removed by rotary evaporation. The aqueous mixture was extracted with ethyl acetate (5 × 100 mL). The combined organic layers were washed with brine, dried with $MgSO_4$, and concentrated to yield 3.8 g (60%) of 3(*Z*)-hexenedioic acid 6-methyl ester (**18**) as a yellow viscous oil: ^{1}H NMR ($CDCl_3$, ppm) 3.1 (m, 4 H, 2 × CH_2), 3.68 (s, 3 H, CH_3), 5.8 (m, 2 H, 2 × CH), 7.5 (very broad, 1 H, COOH). This crude material was carried on to the next step without further purification or characterization.

A mixture of **18** (3.2 g, 20 mmol) and oxalyl chloride (15 mL, 170 mmol) in dry 1,2-dichloroethane (60 mL) was stirred at room temperature for 40 min and then at reflux for 1.5 h. After cooling, the solution was concentrated by distillation to give a dark brown residue that was immediately dissolved in anhydrous CH_2Cl_2 (50 mL) and cooled to 0 °C. $(CH_3)_2NH$ was passed through this solution for 10 min. The resulting cloudy mixture was poured into ice cold 5 N HCl (100 mL). The aqueous mixture was extracted with CH_2Cl_2 (3 × 50 mL). The combined extracts were washed with brine, dried with $MgSO_4$, and concentrated. The residue (1.5 g) was added to a solution of KOH (1.5 g) in 80% aqueous methanol (125 mL) and stirred at room temperature for 2 h. The reaction solution was cooled in an ice bath, acidified with 5 N HCl, and then extracted with $CHCl_3$ (3 × 80 mL). The combined organic layers were washed with brine, dried with $MgSO_4$, and concentrated to yield a yellow viscous oil (0.56 g), which was dissolved in THF (25 mL) and treated with *N*-hydroxysuccinimide (0.5 g, 4.4 mmol) and dicyclohexylcarbodiimide (0.78 g, 3.8 mmol). All solids quickly dissolved, and a white precipitate soon formed. The resulting mixture was stirred at room temperature under N_2 for 2 h. CH_3NH_2·HCl (0.6 g, 8.8 mmol) and triethylamine (1.2 mL, 8.8 mmol) were then added. The milky mixture was stirred overnight at room temperature. Precipitated solids were removed by filtration and washed with THF. The combined filtrate was concentrated and the residue was purified by silica gel column chromatography eluting with 2% (v/v) CH_3OH in $CHCl_3$ to yield 0.12 g of **9** (6% overall) as a colorless liquid: ^{1}H NMR ($CDCl_3$, ppm) 1.62 (s, 3 H, CH_3), 1.66 (s, 3 H, CH_3), 2.82 (d, J = 4.7 Hz, 3 H, CH_3), 2.99 (s, 3 H, CH_3), 3.06 (s, 3 H, CH_3), 3.08 (s, 2 H, CH_2), 3.12 (s, 2 H, CH_2), 7.9 (broad, 1 H, NH); ^{13}C NMR ($CDCl_3$, ppm) 26.27 (CH_3), 31.71 (CH_2), 35.62 (CH_3), 35.76 (CH_2), 37.45 (CH_3), 125.45 (CH=), 126.75 (CH=), 170.98 (2 × C=O); IR (1 mM in CH_2Cl_2, cm^{-1}) 1636, 1654 (shoulder), 1670, 3306, 3455; MS (EI, m/z) 184.1225 (calcd for $C_9H_{16}N_2O_2$ 184.1212).

3,4-Dimethyl-3(*E*)-hexenedioic Acid (20). A solution of 1,3-dithiane (Aldrich, 9.0 g, 75 mmol) in anhydrous THF (250 mL) was cooled to −40 °C under N_2. To this stirred solution was added dropwise a solution of *n*-butyllithium in hexane (35 mL, 2.24 M, 78 mmol) over a period of 30 min. After being stirred for another hour at −15 to −25 °C, the reaction mixture was cooled to −78 °C and a solution of 1,4-dibromo-2,3-dimethyl-3(*E*)-butene[20] (9.0 g, 37 mmol) in anhydrous THF (30 mL)

was added dropwise (~10 min) through a cannula. The resulting yellow mixture was allowed to warm to room temperature over a period of 6 h. Solvent was then removed under reduced pressure. The residue was mixed with water, and undissolved solids were collected by filtration. The isolated white solid was washed with a small amount of ether and dried to yield 8.9 g of 1,4-bis(1,3-dithian-2-yl)-2,3-dimethyl-2(*E*)-butene (74%) as a white solid: mp 137–139 °C; ^{1}H NMR ($CDCl_3$, ppm) 1.78 (s, 6 H, 2 × CH_3), 2.0 (m, 4 H, CH_2), 2.51 (d, J = 7.5 Hz, 4 H, 2 × CH_2), 2.9 (m, 8 H, 4 × SCH_2), 4.20 (t, J = 7.5 Hz, 2 H, 2 × SCHS); ^{13}C NMR ($CDCl_3$, ppm) 19.12 (2 × CH_3), 25.83 (4 × CH_2), 30.62 (4 × SCH_2), 40.21 (2 × CH_2), 46.41 (2 × SCHS), 128.07 (2 × C=); IR (KBr, cm^{-1}) 770, 909, 1178, 1280, 1419, 1442, 2900, 2925; MS (El, m/z) 320.0762 (calcd for $C_{14}H_{24}S_4$ 320.0761).

A slurry of 1,4-bis(1,3-dithian-2-yl)-2,3-dimethyl-2(*E*)-butene (8.6 g, 26 mmol) stirring in CH_3OH (200 mL) was treated with small portions of $PhI(O_2CCF_3)_2$ (40 g total, 93 mmol) at room temperature.[35] All solids quickly dissolved, and an exotherm was observed. After 20 min, TLC (1:4 ethyl acetate/hexane) showed the disappearance of the starting material. The reaction solution was poured into saturated aqueous $NaHCO_3$ (200 mL), and the aqueous solution was extracted with ether (3 × 150 mL). The ether extracts were combined, dried with $MgSO_4$, and concentrated. The crude product was purified by silica gel column chromatography, eluting with 20% (v/v) ethyl acetate in hexane, to yield 5.6 g (90%) of 1,1,6,6-tetramethoxy-3,4-dimethyl-3(*E*)-hexene as a clear liquid: ^{1}H NMR ($CDCl_3$, ppm) 1.74 (s, 6 H, 2 × CH_3), 2.39 (d, J = 5.7 Hz, 4 H, 2 × CH_2), 3.33 (s, 12 H, 4 × OCH_3), 4.42 (t, J = 5.7 Hz, 2 H, 2 × OCHO). Because of its volatility, this material was carried on to the next step without further characterization.

p-TsOH·H_2O (1.0 g) was added to a solution of 1,1,6,6-tetramethoxy-3,4-dimethyl-3(*E*)-hexene (5.6 g, 24 mmol) in THF and water (100 mL, 1:1) at room temperature. The reaction vessel was capped, and the mixture was stirred overnight. The reaction was then quenched by saturated aqueous $NaHCO_3$, and the aqueous mixture was extracted with ether (3 × 100 mL). The ether extracts were combined, washed with brine, dried with Na_2SO_4, and concentrated to yield, after drying on a vacuum line for 5 min, 2.6 g (77%) of 3,4-dimethyl-3(*E*)-hexene-1,6-dial as a slightly yellow liquid: ^{1}H NMR ($CDCl_3$, ppm) 1.76 (s, 6 H, 2 × CH_3), 3.26 (d, J = 2.2 Hz, 4 H, 2 × CH_2), 9.62 (t, J = 2.2 Hz, 2 H, 2 × CHO). Because of its volatility, this material was carried on to the next step without further characterization.

A solution of 3,4-dimethyl-3(*E*)-hexene-1,6-dial (2.6 g, 18 mmol) in acetone (300 mL) was treated with Jones reagent (5.0 g of CrO_3, 4.3 mL of concentrated H_2SO_4, and 36 mL of water) at 0 °C with stirring. A large amount of dark green precipitate formed. The addition of Jones reagent was stopped when the reaction mixture developed a permanent orange-brown color. The mixture was stirred for another 30 min at 0 °C. Ethyl acetate (150 mL) and water (150 mL) were added followed by solid Na_2SO_3 until the organic layer was clear. Acetone and ethyl acetate were removed on a rotary evaporator. The aqueous residue was extracted with ethyl acetate (5 × 50 mL). The combined organic layers were washed with brine, dried with $MgSO_4$, and concentrated to yield 1.3 g of **20** (40%) as a white solid: mp 140–150 °C dec; ^{1}H NMR (DMSO-d_6, ppm) 1.69 (s, 6 H, 2 × CH_3), 2.99 (s, 4 H, 2 × CH_2), 12 (broad s, 2 H, 2 × CO_2H); ^{13}C NMR ($CDCl_3$, ppm) 19.12 (2 × CH_3), 39.66 (2 × CH_2), 125.25 (2 × C=), 172.48 (2 × C=O); IR (KBr, cm^{-1}) 700, 925, 1225, 1331, 1413, 1700, 3000 (very broad); MS (El, m/z) 172.0733 (calcd for $C_8H_{12}O_4$ 172.0736).

***N,N,N',3,4*-Pentamethyl-3(*E*)-hexenediamide (8).** A solution of dicyclohexylcarbodiimide (1.2 g, 5.8 mmol) in anhydrous THF (5 mL) was added, at room temperature with stirring, to a suspension of **20** (1.0 g, 5.8 mmol) in anhydrous THF (6 mL). The precipitate thickened and stirring became difficult. The mixture was allowed to stand at room temperature overnight. The pasty mixture was then treated with 25 mL of 40 wt % aqueous $(CH_3)_2NH$. The mixture was stirred for another day at room temperature. The reaction mixture was then filtered, and the isolated solids were washed with THF. The combined filtrate was evaporated to yield 1.7 g of slightly yellow oil. The ^{1}H NMR spectrum of this material was consistent with a mixture of the mono and bis *N,N*-dimethyl amides of **20**. This crude material (1.7 g) was dissolved in 50 mL of dry THF and treated with *N*-hydroxysuccinimide (1.3 g, 11 mmol) and dicyclohexylcarbodiimide (2.0 g, 9.8 mmol). All solids quickly dissolved, and a white precipitate soon formed. This mixture was stirred at room temperature under N_2 for 2 h. CH_3NH_2·HCl (1.7 g, 25 mmol) and triethylamine (3.4 mL, 25 mmol) were then added. The milky mixture was stirred overnight at room temperature and then filtered, and the isolated solids were washed with THF. The combined filtrate was concentrated, and the residue was purified by silica gel chromatography eluting with 5% (v/v) CH_3OH in $CHCl_3$ to yield 0.39 g (32%) of **8** as a white crystalline solid: mp 83–84 °C; ^{1}H NMR ($CDCl_3$, ppm) 1.62 (s, 3 H, CH_3), 1.66 (s, 3 H, CH_3), 2.82 (d, J = 4.7 Hz, 3 H, NCH_3), 2.99 (s, 3 H, NCH_3), 3.06 (s, 3 H, NCH_3), 3.08 (s, 2 H, CH_2), 3.12 (s, 2 H, CH_2), 7.9 (broad, 1 H, NH); ^{13}C NMR ($CDCl_3$, ppm) 19.67 (CH_3), 20.13 (CH_3), 26.47 (NCH_3), 35.59 (NCH_3), 37.07 (NCH_3), 38.63 (CH_2), 42.36 (CH_2), 127.32 (C=), 128.34 (C=), 170.88 (C=O), 171.10 (C=O); IR (1 mM in CH_2Cl_2, cm^{-1}) 1542, 1606, 1637, 1677, 3302, 3439; MS (El, m/z) 212.1528 (calcd for $C_{11}H_{20}N_2O_2$ 212.1525). Eluting after **8** was 0.30 g (23%) of *N,N,N',N'*,3,4-hexamethyl-3(*E*)-hexenediamide, a white solid: mp 84–86 °C; ^{1}H NMR ($CDCl_3$, ppm) 1.71 (s, 6 H, 2 × CH_3), 2.95 (s, 6 H, 2 × NCH_3), 3.03 (s, 6 H, 2 × NCH_3), 3.19 (s, 4 H, 2 × CH_2); ^{13}C NMR ($CDCl_3$, ppm) 18.46 (2 × CH_3), 35.39 (2 × CH_3), 35.51 (2 × NCH_3), 37.14 (2 × NCH_3), 39.46 (2 × CH_2), 125.30 (2 × C=), 171.17 (2 × C=O); IR (KBr, cm^{-1}) 314, 1137, 1401, 1641, 2935; MS (EI, m/z) 226.1680 (calcd for $C_{12}H_{22}N_2O_2$ 226.1681).

1-(1-Methylcyclopropyl)propane-1,3-diol (23). A solution of Et_2O·BF_3 (15 mL, 120 mmol) in CH_2Cl_2 (50 mL) was added dropwise to **21** (Aldrich, 9.6 mL, 100 mmol) at −30 °C under N_2 with stirring over a period of 30 min. A white precipitate formed. The resulting slurry was stirred at 0 °C for 2 h and then cooled to −78 °C. Ketone **22** (Aldrich, 6 mL, 50 mmol) was added in one portion followed by dropwise addition of *N,N*-diisopropylethylamine (26 mL, 150 mmol) over a period of 30 min.[36] The reaction was stirred at −78 °C for another hour and then poured into saturated aqueous $NaHCO_3$ (400 mL). The aqueous mixture was extracted with CH_2Cl_2 (3 × 150 mL). The combined organic layers were washed with ice cold 1 N H_2SO_4, ice water, and brine, dried with $MgSO_4$, and evaporated to yield 8.5 g (crude, quantitative yield) of a yellow liquid, which was used directly without purification. A sample for analysis was purified by silica gel column chromatography eluting with 20% (v/v) ethyl acetate in hexane to yield two products in ~1:2 ratio. The first eluted was 1-methylcyclopropyl 2,2-dimethoxyethyl ketone, obtained as a slightly yellow liquid: ^{1}H NMR ($CDCl_3$, ppm) 0.74 (m, 2 H, cyclopropyl), 1.25 (m, 2 H, cyclopropyl), 1.33 (s, 3 H, CH_3), 2.64 (d, J = 5.4 Hz, 2 H, CH_2), 3.37 (s, 6 H, 2 × OCH_3), 4.81 (t, J = 5.4 Hz, 1 H, CH); ^{13}C NMR ($CDCl_3$, ppm) 17.07 (CH_2), 19.15 (CH_3), 26.82 (C), 40.98 (CH_2), 53.95 (CH_3), 102.22 (CH), 207.63 (C=O); IR (neat, cm^{-1}) 754, 855, 1055, 1384, 1686, 2833, 2937; MS (EI, m/e) 172.1098 (calcd for $C_9H_{16}O_3$ 172.1099). The second to elute was 1-methylcyclopropyl (1,3-dioxolan-2-yl)methyl ketone, obtained as a slightly yellow liquid: ^{1}H NMR ($CDCl_3$ ppm) 0.76 (m, 2 H, cyclopropyl), 1.30 (m, 2 H, cyclopropyl), 1.34 (s, 3 H, CH_3), 2.72 (d, J = 5.0 Hz, 2 H, CH_2), 3.9 (m, 4 H, OCH_2CH_2O), 5.25 (t, J = 5.0 Hz, 1 H, CH); ^{13}C NMR ($CDCl_3$, ppm) 17.67 (CH_2), 19.39 (CH_3), 27.14 (C), 42.01 (CH_2), 64.84 (CH_2), 101.45 (CH), 207.86 (C=O); IR (neat, cm^{-1}) 759, 855, 1035, 1136, 1391, 1685, 1737, 2888, 2967; MS (EI, m/e) 170.0955 (calcd for $C_9H_{14}O_3$ 172.0943).

A solution of $LiAlH_4$ in ether (1 M, 35 mL, 35 mmol) was added slowly to a stirred solution of the crude mixture of the two ketones described above (8.5 g, ~1:2 mixture, ~50 mmol total) in THF at 0 °C under N_2. The reaction was stirred for another hour at 0 °C and quenched by cautious addition of freshly made saturated aqueous Na_2SO_4. The white precipitated solids were removed by filtration, and the filtrate was concentrated to yield 8.5 g (crude, quantitative yield) of yellow viscous oil. This crude product, which contained 1-(1-methylcyclopropyl)-3,3-dimethoxypropan-1-ol and 1-(1-methylcyclopropyl)-2-(1,3-dioxolan-2-yl)ethanol (~1:2), was not easily separable on a silica gel column. The same reaction was also carried out separately on smaller scale with the pure ketones to yield both products in pure form. 1-(1-Methylcyclopropyl)-2-(1,3-dioxolan-2-yl)ethanol (95%) was obtained as a colorless viscous liquid: ^{1}H NMR ($CDCl_3$ ppm) 0.4 (m, 4 H, cyclopropyl), 1.05 (s, 3 H, CH_3), 1.95 (m, 2 H, CH_2), 2.66 (d, J = 1.6 Hz, 1 H, OH), 3.17 (td, J = 6.1, 1.6 Hz, 1 H, OCH), 3.9 (m, 4 H, OCH_2CH_2O), 5.04 (t, J = 4.6 Hz, 1 H, CH); ^{13}C NMR ($CDCl_3$, ppm) 10.29 (CH_2), 12.47 (CH_2), 17.41 (CH_3), 20.08 (C), 37.70 (CH_2), 64.58 (CH_2), 64.87 (CH_2), 74.37 (CH), 103.46 (CH); IR (neat, cm^{-1}) 757, 1023, 1072, 1142, 1415, 2886, 2959, 3073, 3482 (broad); MS (EI, m/e) 171.1019 (calcd for $C_9H_{15}O_3$ (M^+ − H) 171.1021). 1-(1-Methylcyclopropyl)-2,2-dimethoxypropan-1-ol (95%) was obtained as a colorless viscous liquid: ^{1}H NMR ($CDCl_3$ ppm) 0.4 (m, 4 H, cyclopropyl), 1.04 (s, 3 H, CH_3), 1.86 (m, 2 H, CH_2), 2.65 (broad, 1 H, OH), 3.06 (dd, J = 8.6, 3.8 Hz, 1 H, OCH), 3.35 (s, 3 H, OCH_3), 3.38 (s, 3 H, OCH_3), 4.58 (t, J = 5.7 Hz, 1 H, CH); ^{13}C NMR ($CDCl_3$, ppm) 10.36 (CH_2), 12.32 (CH_2), 17.52 (CH_3), 20.16 (C), 36.73 (CH_2), 52.67 (CH_3), 53.78 (CH_3), 74.88 (CH), 103.83 (CH); IR (neat, cm^{-1}) 893, 1059, 1129, 1383, 1457, 2958, 3073, 3469 (broad); MS (El, m/e) 143.1069 (calcd for $C_8H_{15}O_2$ (M^+ − CH_3O) 143.1072).

(35) Stork, G.; Zhao, K. *Tetrahedron Lett.* **1989**, *30*, 287.

(36) For a leading reference on this methodology, see: Mock, W. L.; Tsou, H.-R. *J. Org. Chem.* **1981**, *46*, 2557.

A solution of 1-(1-methylcyclopropyl)-3,3-dimethoxypropan-1-ol and 1-(1-methylcyclopropyl)-2-(1,3-dioxolan-2-yl)ethanol (7.0 g, ~1:2 mixture, ~40 mmol) in THF (200 mL) and 3 N HCl (100 mL) was stirred at room temperature for 2 h. The solution was cooled to 0 °C, and solid $NaHCO_3$ (~25 g) was added in small portions followed by $NaBH_4$ (3.2 g, 80 mmol) in small portions over 30 min. The reaction mixture was stirred for another hour at 0 °C and allowed to warm to room temperature. The reaction mixture was extracted with ethyl acetate (5 × 100 mL). The combined organic extracts were washed with brine, dried with $MgSO_4$, and concentrated. The crude product was purified by silica gel column chromatography eluting with 5% (v/v) CH_3OH in $CHCl_3$ to yield 4.4 g (83%) of **23** as a colorless viscous liquid: ^{1}H NMR ($CDCl_3$ ppm) 0.4 (m, 4 H, cyclopropyl), 1.06 (s, 3 H, CH_3), 1.8 (m, 2 H, CH_2), 2.58 (broad, 1 H, OH), 2.91 (broad, 1 H, OH), 3.11 (dd, J = 9.6, 2.9 Hz, 1 H, OCH), 3.8 (m, 2 H, CH2O); ^{13}C NMR $CDCl_3$, ppm) 10.51 (CH_2), 12.21 (CH_2), 17.40 (CH_3), 20.47 (C), 35.40 (CH_2), 61.55 (CH_2), 78.38 (CH); IR (neat, cm^{-1}) 756, 1058, 1429, 2956, 3074, 3344 (broad); MS (El, m/e) 112.0888 (calcd for $C_7H_{12}O$ ($M^+ - H_2O$) 112.0888).

6-Bromo-4-methyl-3(*E*)-hexen-1-ol (24). To magnesium turnings (2.0 g, excess) stirred in anhydrous ether (100 mL) was added 1,2-dibromoethane (3.0 mL, 34 mmol) under N_2. After visible reaction had ceased, the supernatant was transferred into a solution of **23** (3.0 g, 23 mmol) in anhydrous ether (50 mL). The resulting mixture was stirred at reflux overnight and then cooled to −20 °C. HBr (48%, 7.5 mL) was added dropwise, and the reaction mixture was stirred for another 30 min while it was allowed to warm to room temperature. The precipitated solids were removed by filtration and washed with ether. The combined filtrate was washed with saturated aqueous $NaHCO_3$ (3 × 100 mL) and brine. The organic solution was dried with $MgSO_4$ and concentrated to give crude **24** (3.1 g, 69%) as a brown liquid: ^{1}H NMR ($CDCl_3$, ppm) 2.95 (s, 3 H, CH_3), 3.02 (s, 3 H, CH_3), 3.14 (m, 4 H, 2 × CH_2), 3.69 (s, 3 H, CH_3), 5.8 (m, 2 H, 2 × CH). This material was used for the next reaction directly without further purification or characterization.

***N,N,N'*,3-Tetramethyl-3(*E*)-hexenediamide (7).** Cesium acetate (9.0 g, 47 mmol) was added to a solution of crude **24** (3.1 g, 16 mmol) in DMF (100 mL). The mixture was stirred at 70 °C for 40 h and then cooled to room temperature. Water (200 mL) was added to the reaction mixture, and the resulting aqueous mixture was extracted with ethyl acetate (8 × 100 mL). The organic layers were combined, concentrated to ~300 mL, washed with 1 N $NaHCO_3$ (3 × 100 mL) and brine (200 mL), dried with $MgSO_4$, and concentrated. The crude product was purified by silica gel column chromatography eluting with ethyl acetate and hexane (1:1) to yield 1.0 g of 6-acetoxy-4-methyl-3(*E*)-hexen-1-ol (35% from **23**) as a colorless liquid: ^{1}H NMR ($CDCl_3$ ppm) 1.69 (s, 3 H, CH_3), 1.9 (broad, 1 H, OH), 2.04 (s, 3 H, CH_3), 2.3 (m, 2 H), 2.33 (t, J = 6.9 Hz, 2 H, CH_2), 3.26 (t, J = 6.5 Hz, CH_2), 4.16 (t, J = 6.9 Hz, CH_2), 5.22 (tq, J = 6.8, 1.2 Hz, =CH); ^{13}C NMR ($CDCl_3$, ppm) 16.18 (CH_3), 21.02 (CH_3), 31.43 (CH_2), 38.64 (CH_2), 62.14 (CH_2O), 62.76 (CH_2O), 122.74 (CH=), 134.30 (C=), 171.17 (C=O); IR (neat, cm^{-1}) 756, 1045, 1245, 1368, 1435, 1669, 1739, 2937, 3410 (broad); MS (El, m/e) 142.0991 (calcd for $C_8H_{14}O_2$ ($M^+ - CH_2O$) 142.0994).

Jones reagent (5.0 g of CrO_3, 4.3 mL of concentrated H_2SO_4, and 36 mL of water) was added dropwise to a vigorously stirred solution of 6-acetoxy-4-methyl-3(*E*)-hexen-1-ol (0.9 g, 5.2 mmol) in acetone (130 mL) at 0 °C over a period of 30 min. A dark green precipitate formed immediately. The resulting mixture was stirred at 0 °C for another 30 min. A small amount of Jones reagent was added to maintain the orange-brown color. The reaction mixture was quenched by adding water (100 mL), and then ethyl acetate (150 mL) was added followed by Na_2SO_3 in small portions until the organic layer was clear. The mixture was concentrated to ~100 mL by rotary evaporation. The remaining aqueous mixture was extracted with ethyl acetate (5 × 100 mL). The organic extracts were washed with brine, dried with $MgSO_4$, and concentrated to yield 0.88 g of 6-acetoxy-4-methyl-3(*E*)-hexenoic acid (90%) as a slightly yellow liquid: ^{1}H NMR ($CDCl_3$, ppm) 1.68 (s, 3 H, CH_3), 2.04 (s, 3 H, CH_3), 2.36 (t, J = 6.8 Hz, 2 H, CH_2), 3.11 (d, J = 7.1 Hz, CH_2), 4.17 (t, J = 6.8 Hz, CH_2), 5.39 (tq, J = 7.1, 1.2 Hz, =CH), 8.4 (very broad, 1 H, COOH); ^{13}C NMR ($CDCl_3$, ppm) 16.18 (CH_3), 20.84 (CH_3), 33.29 (CH_2), 38.30 (CH_2), 62.50 (CH_2O), 117.73 (CH), 135.35 (C=), 171.24 (C=O), 177.55 (C=O); IR (neat, cm^{-1}) 1043, 1245, 1387, 1726, 2965, 3467 (very broad); ME (El, m/e) 126.0668 (calcd for $C_7H_{10}O_2$ ($M^+ - C_2H_4O_2$) 126.0681).

Concentrated H_2SO_4 (5 drops) was added to a solution of 6-acetoxy-4-methyl-3(*E*)-hexenoic acid (0.3 g, 1.6 mmol) in CH_3OH (20 mL). The acidified solution was stirred at room temperature for 8 h and then carefully poured into 1 N $NaHCO_3$ (50 mL). This aqueous mixture was extracted with ether (4 × 25 mL). The combined ether extract was washed with brine, dried with $MgSO_4$, and concentrated to yield 0.172 g (68%) of methyl 6-hydroxy-4-methyl-3(*E*)-hexenoate as a slightly yellow liquid: ^{1}H NMR ($CDCl_3$ ppm) 1.67 (br s, 3 H, CH_3), 1.9 (br s, 1 H, OH), 2.31 (t, J = 6.3 Hz, 2 H, CH_2), 3.10 (d, J = 5.9 Hz, 2 H, CH_2), 3.69 (br s, 3 H, CH_3), 3.70 (t, J = 6.3 Hz, 2 H, CH_2), 5.43 (tq, J = 5.9, 1.3 Hz, 1 H, CH); ^{13}C NMR ($CDCl_3$, ppm) 16.20 (CH_3), 33.34 (CH_2), 42.40 (CH_2), 51.85 (CH_3), 60.08 (CH_2), 118.48 (=CH), 135.76 (=C), 172.67 (C=O); IR (neat, cm^{-1}) 1045, 1164, 1437, 1739, 2953, 3440 (broad); MS (El, m/e) 140.0186 (calcd for $C_7H_{14}O_2$ 140.0181).

To a stirred solution of methyl 6-hydroxy-4-methyl-3(*E*)-hexenoate (57 mg, 0.36 mmol) in dry THF (5 mL) was added triethylamine (75 mL, 0.54 mmol) and chlorotrimethylsilane (60 mL, 0.47 mmol). A white precipitate formed immediately. The resulting mixture was stirred at room temperature overnight and then poured into water (15 mL). This aqueous mixture was extracted with ether (3 × 15 mL). The combined ether layers were washed with brine, dried with $MgSO_4$, and concentrated to yield 70 mg (84%) of a slightly yellow liquid: ^{1}H NMR ($CDCl_3$ ppm) 0.08 (s, 9 H, $SiCH_3$), 1.63 (br s, 3 H, =CCH_3), 2.24 (t, J = 7.2 Hz, 2 H, CH_2), 3.03 (d, J = 7.1 Hz, 2 H, CH_2C=O), 3.65 (s, 3 H, OCH_3), 3.6–3.7 (m, 2 H, CH_2OSi), 5.34 (m, 1 H, =CH); ^{13}C NMR ($CDCl_3$, ppm) −0.53 (CH_3), 16.70 (CH_3), 33.52 (CH_2), 42.57 (CH_2), 51.67 (CH_3), 61.46 (CH_2), 117.46 (CH), 136.05 (C), 172.63 (C=O); IR (neat, cm^{-1}) 748, 842, 1092, 1251, 1437, 1742, 2955; MS (El, m/e) 230.1346 (calcd for $C_{11}H_{22}O_3Si$ 230.1338).

NOE measurements were carried out with this compound to assign double-bond stereochemistry. Irradiated at 5.34 ppm (H_a), observed: H_b, 1.0%; H_c, 1.8%; H_d, 0.2%. Irradiated at 3.00 ppm (H_b), observed: H_a, 2.2%; H_c, 0.4%; H_d, 1.7%. Irradiated at 2.24 ppm (H_c), observed: H_a, 6.1%; H_b, −1.3%; H_d, 0.4%. Irradiated at 1.63 ppm (H_d), observed: H_a, 0.9%; H_b, 3.3%; H_c, 2.3%.

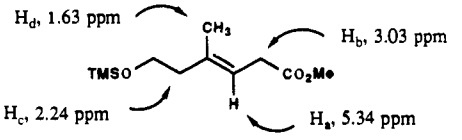

Jones reagent (5.0 g of CrO_3, 4.3 mL of concentrated H_2SO_4, and 36 mL of water) was added dropwise to a vigorously stirred solution of methyl 6-hydroxy-4-methyl-3(*E*)-hexenoate (0.9 g, 5.2 mmol) in acetone (50 mL) at 0 °C over a period of 15 min. A dark green precipitate formed immediately. The resulting mixture was stirred at 0 °C for 1 h. During this time, a small amount of Jones reagent was added to maintain the orange-brown color. The reaction mixture was quenched by adding water (50 mL), and then ethyl acetate (100 mL) was added followed by Na_2SO_3 in small portions until the organic layer was clear. The mixture was concentrated to ~50 mL by rotary evaporation. The remaining aqueous mixture was extracted with ethyl acetate (5 × 50 mL). The combined organic layers were washed with brine, dried with $MgSO_4$, and concentrated to yield 0.25 g (90%) of 5-(methoxycarbonyl)-3-methyl-3-(*E*)-pentenoic acid as a slightly yellow liquid: ^{1}H NMR ($CDCl_3$ ppm) 1.75 (s, 3 H, CH_3), 3.10 (s, 2 H, CH_2), 3.12 (d, J = 6.7 Hz, 2 H, CH_2), 3.69 (s, 3 H, OCH_3), 5.54 (tq, J = 6.7, 1.4 Hz, 1 H, =CH), 10.1 (very broad, 1 H, COOH); ^{13}C NMR ($CDCl_3$, ppm) 16.41 (CH_3), 33.42 (CH_2), 44.37 (CH_2), 51.82 (OCH_3), 121.08 (CH), 131.54 (CH), 172.21 (C=O), 177.26 (C=O); IR (neat, cm^{-1}) 1017, 1169, 1315, 1437, 1735, 2956, 3193 (very broad); MS (EI, m/e) 172.0734 (calcd for $C_8H_{12}O_4$ 172.0736).

A solution of 5-(methoxycarbonyl)-3-methyl-3(*E*)-pentenoic acid (150 mg, 0.9 mmol) in 10 mL of dry THF was treated with 1-[3-(dimethylamino)propyl]-3-ethylcarbodiimide hydrochloride (190 mg, 1.0 mmol), triethylamine (210 mL, 1.5 mmol), and $(CH_3)_2NH$·HCl (125 mg, 1.5 mmol). All solids quickly dissolved, and a white precipitate soon formed. The resulting mixture was stirred under N_2 overnight at room temperature. Solvent was removed, and the residue was taken up in $CHCl_3$ (15 mL). The resulting solution was washed with 1 N HCl, 1 N $NaHCO_3$, and brine, dried with $MgSO_4$, concentrated on a rotary evaporator, and further dried on a vacuum line to yield 100 mg (58%) of *N,N*,3-trimethyl-5-(methoxycarbonyl)-3(*E*)-pentenamide as a colorless liquid: ^{1}H NMR ($CDCl_3$ ppm) 1.71 (s, 3 H, CH_3), 2.96 (s, 3 H, NCH_3), 3.01 (s, 3 H, NCH_3), 3.12 (m, 4 H, 2 × CH_2), 3.68 (s, 3 H, OCH_3), 5.41 (m, 1 H, =CH). This material was used for the next reaction without further purification or characterization.

A solution of *N,N*,3-trimethyl-5-(methoxycarbonyl)-3(*E*)-pentenamide in 1 N NaOH (2 mL) and THF (2 mL) was stirred at room temperature for 30 min. The mixture was washed with ether, and the remaining aqueous solution was acidified carefully with concentrated HCl at 0 °C and then extracted with $CHCl_3$ (3 × 10 mL). The combined $CHCl_3$ washes were shaken with brine, dried with Na_2SO_4, and concentrated to yield 50 mg of slightly yellow liquid. This crude acid (40 mg, 0.2 mmol) was dissolved in CH_2Cl_2 (5 mL) and then treated with *N*-hydroxysuccinimide (33 mg, 0.28 mmol) and dicyclohexylcarbodiimide (50 mg, 0.25 mmol). All solids quickly dissolved, and a white precipitate soon

formed. The resulting mixture was stirred at room temperature under N_2 for 2 h. CH_3NH_2·HCl (44 mg, 0.64 mmol) and triethylamine (90 mL, 0.64 mmol) were then added. The milky mixture was stirred overnight at room temperature. Precipitated solids were removed by filtration and washed with THF. The combined filtrate was concentrated and the residue was purified by silica gel column chromatography eluting with 4% (v/v) CH_3OH in $CHCl_3$ to yield 30 mg (70%) of **7** as a colorless liquid: ^{1}H NMR ($CDCl_3$ ppm) 1.67 (s, 3 H, CH_3), 2.81 (d, J = 4.7 Hz, 3 H, NCH_3), 2.98 (s, 3 H, NCH_3), 3.03 (d, J = 6.5 Hz, 2 H, CH_2), 3.04 (s, 3 H, NCH_3), 3.08 (s, 2 H, CH_2), 5.35 (t, J = 7.3 Hz, 1 H, =CH), 7.2 (broad, 1 H, NH); ^{13}C NMR ($CDCl_3$, ppm) 17.09 (CH_3), 26.41 (CH_3), 35.62 (CH_3), 35.80 (CH_2), 37.24 (CH_3), 43.39 (CH_2), 121.85 (CH), 135.95 (C), 171.19 (C=O), 171.47 (C=O); IR (1 mM in CH_2Cl_2, cm^{-1}) 1638, 1656, 1673 (shoulder), 3313, 3453; MS (EI, m/e) 198.1365 (calcd for $C_{10}H_{18}N_2O_2$ 198.1369).

***N*-Methylcyclopentanecarboxamide (25).** To a solution of cyclopentanecarboxylic acid (0.57 g, 5.0 mmol) in 30 mL of freshly distilled THF was added *N*-hydroxysuccinimide (0.86 g, 7.5 mmol) and then dicyclohexylcarbodiimide (1.3 g, 6.2 mmol). All solids quickly dissolved, and a white precipitate soon developed. After 1 h, CH_3NH_2·HCl (1.0 g, 15 mmol) and Et_3N (2.0 mL, 15 mmol) were added. This mixture was allowed to stir overnight, and the suspended solids were then removed by filtration and washed with THF. The combined filtrate was concentrated, and the residue was chromatographed on silica gel, eluting with 5% (v/v) CH_3OH in $CHCl_3$ to yield 0.5 g (79%) of **25** as a white crystalline solid: mp 56–58 °C; ^{1}H NMR ($CDCl_3$, ppm) 1.5–2.0 (m, 8 H, CH_2), 2.5 (m, 1 H, CH), 2.80 (d, J = 4.8 Hz, 2 H, NCH_3), 5.75 (br m, 1 H, NH); IR (CH_2Cl_2, cm^{-1}) 1224, 1276, 1412, 1452, 1469, 1523, 1562, 1667, 2871, 2914, 1961, 3056, 3459; MS (EI, m/z) 127.0996 (calcd for $C_7H_{13}NO$ 127.0997).

***N*-Methyl-3(*E*)-hexenamide (26).** To a solution of 3(*E*)-hexenoic acid (Aldrich, 1.0 g, 8.5 mmol) in 50 mL of freshly distilled THF were added *N*-hydroxysuccinimide (1.4 g, 12 mmol) and then dicyclohexylcarbodiimide (2.1 g, 10 mmol). All solids quickly dissolved, and a white precipitate soon developed. After 1 h, CH_3NH_2·HCl (1.7 g, 25 mmol) and Et_3N (3.5 mL, 25 mmol) were added. This mixture was allowed to stir overnight, and the suspended solids were then removed by filtration and washed with THF. The combined filtrate was concentrated, and the residue was chromatographed on silica gel, eluting with 1–5% (v/v) CH_3OH in $CHCl_3$ to yield 1.0 g (90%) of **26** as a colorless oil: ^{1}H NMR ($CDCl_3$, ppm) 1.01 (t, J = 7.4 Hz, 3 H, CH_3), 2.08 (m, 2 H, CH_2), 2.80 (d, J = 4.9 Hz, 3 H, NCH_3), 2.94 (br d, J = 7.8 Hz, 2 H, CH_2), 5.5–5.7 (m, 2 H, =CH), 5.71 (br, 1 H, NH); IR (CH_2Cl_2, cm^{-1}) 1278, 1414, 1435, 1462, 1529, 1662, 1671, 2851, 2875, 2919, 2935, 2966, 3049, 3054, 3442, 3453; MS (EI, m/z) 127.0994 (calcd for $C_7H_{13}NO$ 127.0997).

***N*,*N*-Dimethyl-*N*'-(1-adamantyl)-3(*E*)-hexenediamide (27).** To a stirred suspension of 3(*E*)-hexenedioic acid (Aldrich, 4.8 g, 33 mmol) in 50 mL of freshly distilled THF at 0 °C was added 1-ethyl-3-[3-(dimethylamino)propyl]carbodiimide (5.5 g, 28 mmol). The mixture was allowed to warm to room temperature and stir under N_2 overnight. The mixture was then cooled to 0 °C, and 70 mL of 40 wt % aqueous $(CH_3)_2NH$ was added. The resulting dark brown reaction mixture was allowed to warm to room temperature and stir for a day. The mixture was then recooled to 0 °C and carefully acidified with concentrated HCl. This mixture was extracted five times with 50 mL of $CHCl_3$. The organic layers were combined, washed with brine, dried over $MgSO_4$, and concentrated to yield 2.9 g of a slightly yellow residue that solidified upon standing. A portion (0.5 g) of this crude acid amide was dissolved in 30 mL of freshly distilled THF, and *N*-hydroxysuccinimide (0.5 g, 4.2 mmol) and then dicyclohexylcarbodiimide (0.75 g, 3.6 mmol) were added. All solids quickly dissolved, and a white precipitate soon developed. After 1 h, 1-adamantylamine (0.8 g, 5.0 mmol) was added. This mixture was allowed to stir overnight, and the suspended solids were then removed by filtration and washed with THF. The combined filtrate was concentrated, and the residue was chromatographed on silica gel eluting with 3.5% (v/v) CH_3OH in $CHCl_3$. Partially purified material was rechromatographed, eluting with 2% (v/v) CH_3OH in $CHCl_3$ to yield 0.46 g (52%) of **27** as a crystalline solid: mp 124–126 °C; ^{1}H NMR ($CDCl_3$, ppm) 1.67, 2.00, 2.06 (br singlets, 15 H, adamantyl), 2.92 (br d, J = 5.8 Hz,,2 H, CH_2) 2.95 (s, 3 H, CH_3), 3.02 (s, 3 H, CH_3), 3.12 (br d, J = 5.6 Hz, 2 H, CH_2), 5.57 (br, 1 H, NH), 5.67 (m, 2 H, =CH); IR (CH_2Cl_2, cm^{-1}) 1278, 1297, 1309, 1345, 1360, 1400, 1414, 1454, 1469, 1512, 1642, 1673, 2853, 2911, 2979, 3025, 3050, 3324 (br), 3424; MS (EI, m/z) 304.2151 (calcd for $C_{18}H_{28}N_2O_2$ 304.2151).

Growth of Crystals for Diffraction Studies. Colorless plates of **8** and **27** were obtained by vapor diffusion of hexane into $CHCl_3$ solutions at room temperature.

Acknowledgment. This work was supported by the National Science Foundation (CHE-9014488). We are grateful to G. Dado and R. Gardner for technical assistance and to Professor Craig Wilcox for helpful comments. G.B.L. thanks B,P,-America for fellowship support. S.H.G. thanks the Searle Scholars Program, the American Cancer Society (Junior Faculty Research Award), the National Science Foundation Presidential Young Investigator Program, Marion Merrell Dow Inc., and Merck Sharp and Dohme for support. The FT-IR was purchased with funds provided by the Office of Naval Research.

Supplementary Material Available: Listings of crystallographic details for **8** and **27**, including tables of atomic coordinates and bond lengths and angles (18 pages). Ordering information is given on any current masthead page.